Norwegian University of Life Sciences

**Master's Thesis 2019 60 ECTS**
Faculty of Biosciences

# Non- invasive prediction of vertebral deformities and mineral deposition using Computed Tomography (CT) for the advancement in breeding of Atlantic salmon

Valerie Chidakwa
Master of Science Animal Breeding and Genetics

# Non- invasive prediction of vertebral deformities and mineral deposition using Computed Tomography (CT) for the advancement in breeding of Atlantic salmon

**Master of Science in Animal Breeding and Genetics**

Master thesis
60 credits

By

**Valerie Chidakwa**

Supervisors

Prof. Turid Mørkøre
Dr. Anne Kettunen

Department of Animal and Aquaculture Sciences

**Norwegian University of Life Science (NMBU)**
**Faculty of Biosciences**
Post Box 5003
1432 Ås

December 2019

# Acknowledgements

I would like to thank those, whom without their contribution, I would not have managed to successfully complete my study. From the scientists and research technicians at Nofima As, Sundalsøra and Salmobreed I am eternally grateful. It has been a long journey with this study, but I am grateful for the opportunity from Nofima AS to undertake my thesis with them under the continued support of my supervisor, Professor Turid Møkøre. Your patience, assistance and confidence in my capabilities have continued to nurture my passion for research.

I would like to thank my friends who encouraged me and kept me motivated while I brainstormed unimaginable ideas to them. I appreciate the random ear to listen when I was panicking.

I would like to thank my family for their regular check-ups on me and words of encouragement. It is tough being away from home and missing a lot of milestones back home because of pursuit of further education, but I am glad that through constant communication I have successfully endured and risen above.

# Dedication

I dedicate this study to my mum, Lucy Gondokondo. So many years away from home and you have been a constant pillar of strength and encouragement in my journey. This one is for you.

TABLE OF CONTENTS

ACKNOWLEDGEMENTS ..... I

DEDICATION ..... II

ABSTRACT ..... V

1 INTRODUCTION ..... 6

2 BACKGROUND ..... 8

2.1 ATLANTIC SALMON ..... 8
*2.1.1 Atlantic salmon lifecycle* ..... *9*
2.2 QUALITY ..... 12
2.3 BONE STRUCTURE/ SKELETON ..... 13
2.4 DEFORMITIES ..... 17
*2.4.1 Vertebral fusion* ..... *17*
*2.4.2 Compression* ..... *17*
*2.4.3 Jaw deformity* ..... *18*
2.5 CAUSES OF DEFORMITIES ..... 18
*2.5.1 Water Temperature* ..... *21*
*2.5.2 Velocity of water current* ..... *21*
*2.5.3 Tank Colour* ..... *21*
*2.5.4 Nutritional factors* ..... *22*
*2.5.5 Abnormal swim bladder* ..... *23*
*2.5.6 Other Factors* ..... *23*
2.6 RADIOGRAPHY ..... 23
*2.6.1 Computed Tomography (CT)* ..... *25*
*2.6.2 Principles of CT scanning* ..... *25*
*2.6.3 CT image reconstruction* ..... *29*
2.7 BONE QUALITY ..... 32
*2.7.2 Bone density measurement* ..... *33*
*2.7.3 Imagej* ..... *34*
2.8 FISH MATERIAL FOR RADIOGRAPHY ..... 38
*2.8.1 Fixed samples* ..... *38*
*2.8.2 Frozen samples* ..... *38*
2.9 HERITABILITY ..... 38
*2.9.1 Estimating heritability* ..... *39*
*2.9.2 Heritability can be further classified into:* ..... *43*
*2.9.3 Genetic correlation* ..... *44*

3 MATERIALS AND METHODS ..... 45

3.1 FISH MATERIAL ..... 45
3.2 CT SCANNING AND IMAGE ANALYSIS ..... 45
3.3 PHYSICAL ANALYSIS ..... 49
3.4 FILLET FAT CONTENT ..... 50
3.4 STATISTICAL CALCULATIONS ..... 50
HERITABILITY ..... 51

4 RESULTS ..... 52

4.2 DEFORMITY ..... 54
4.3 COLORIMETRIC ANALYSIS ..... 54

4.4 HERITABILITY ..... 65
5 DISCUSSION ..... 70
6 CONCLUSION ..... 73
7 REFERENCES ..... 74
8 APPENDICES ..... 82
APPENDIX A ..... 82
APPENDIX B ..... 86
APPENDIX C ..... 87
APPENDIX D ..... 91
APPENDIX E ..... 93
APPENDIX F ..... 94

# Abstract

The aim of this thesis was to develop a method for determination of vertebral deformities and mineral deposition in the skeleton of gutted Atlantic salmon using a novel non-invasive method based on computer tomography (CT). Furthermore, to estimate heritabilities for vertebra deformity and mineral deposition in salmon skeleton.

An experiment was carried out with one thousand one hundred and seventy-six whole and dead fish with known pedigree from the breeding company SalmoBreed AS, Norway: 100 full- and half-sib families (year-class 2016). Colorimetric values of the skeleton were obtained through analysis of CT images with an application called ImageJ after the images had been divided into five main regions along the vertebral column (Region A- E). In addition, soft bone, strong bone (jaw) and skeleton muscle were analysed. The values obtained in ImageJ were transformed to the Cie-Lab colour space because it is closer to what the human eye can see. The L* and b* values were focused on in the analysis as the L* value and a* value were highly correlated (r =-0.998).

The L* value (lightness) and b*value (bluish colour) differed significantly between the eight anatomical regions of the whole fish (R=86.3% and 63.1%, respectively), indicating significant difference in mineral content. From this study, the L* and b* values indicated decreasing mineral concentration from head to tail. Mineralization was highest in the jaw whereas the soft bones attaching the dorsal fin to the fillet and skeletal muscle had the lowest mineral concentration.

Bone mineral densities of the different regions of the fish from the L* and b* values as estimated in ASReml are moderately heritable. The average heritability for the L* values was 0.26, which is considered significant and moderate. The average heritability for the b* values was 0.24. The region of the vertebral column showing the highest heritability was the area below the dorsal fin (region C: $h^2$=0.32 for the L*value and $h^2$=0.33 for the b*value). Fillet deformity, vertebral deformity and the number of vertebrae affected have heritability's of 0.08, 0.05 and 0.04 respectively.

In the end, a novel method for predicting Atlantic salmon bone mineralization was developed based on highly sensitive and advanced equipment-Computed Tomography and image analyses (Cie-lab colorimetric parameters).

# 1 Introduction

Human beings are omnivorous in nature meaning they have adapted to a varied diet. This diet differs amongst different cultures and amongst the variety of foods that are consumed daily by humans, fish is one of them. On a global basis, seafood consumption has more than doubled in the past 50 years, to over 20 kg per capita per year in 2014, putting stress on the sustainability of fishing (EU JRC, 2018). During the last three decades, capture fisheries production increased from 69 million to 93 million tons; during the same time, world aquaculture production increased from 5 million to 63 million tons (FishStat, Accessed 2019). The seafood supply from aquaculture is projected to supply over 60 percent of fish destined for direct human consumption in 2030 (FAO, 2013).

Atlantic salmon is classified as a white meat specie. Currently, many people prefer to consume white meat over red meat. It is generally allowed in all cultures and religions and has minimum allergens (Oldenbroek & Waaij, 2014). Fish such as salmon is usually low in saturated fats, carbohydrates, and cholesterol and provides not only high-value protein but also a wide range of essential micronutrients, including various vitamins, minerals, and polyunsaturated omega-3 fatty acids (FAO, 2012).

Farming of Atlantic salmon has become an important industry in several countries, and breeding programs have been implemented to improve genetic performance and adaptation to farm environments (Gjøen & Bentsen, 1997). In fact, selection experiments started already in the 1970's. The selective breeding of families, the genetic material selected and subsequent adaptation to both the needs of the consumer and farmers was established by genetic researchers from the first 12 rivers of the 40 different rivers sampled along the coast of Norway (Gjedrem, et al., 1991).

Productivity in the aquaculture industry has been increased from 1970 to 2010 by selective breeding with advances in reduced production times [fresh water (egg-smolt) phase from 16 months down to 8 months and seawater (smolt-harvest) phase from 24 months down to 12 months]; late sexual maturation age; efficient feed conversion rate (less feed per kilogram meat produced); disease resistance (especially from the viral infectious pancreatic necrosis (IPN)); good quality fillet (pigmentation and fat score). Apart from genetic gain, standard operations have been continuously developed, with an increase in the knowhow and experience of farming Atlantic salmon through selective breeding (Gjedrem, et al., 1991).

A reduction in consumer acceptance of fish and/or fish products can be due to a prevalence in skeletal deformities in the fish. Hatchery productions have been downgraded by the level of skeletal deformities as a contributing factor to high economy for producers. This is because fish with skeletal deformities have a higher mortality rate than those without. They are not satisfying to the eye and are shunned upon by consumers. Skeletal deformities come about as a combination of one or more bone disorders (Helland, et al., 2005). Possible causes of skeletal deformities and the types of skeletal deformities will be discussed in detail in the next chapter.

The aim of this project is to measure the slaughter quality traits of gutted Atlantic salmon with focus on non-invasive determination of vertebra deformities and mineral deposition in the salmon skeleton using a novel non-invasive method based on computed tomography (CT). Furthermore, to estimate heritability's for vertebral deformity and mineral deposition based on the CT measurements.

# 2 Background

## 2.1 Atlantic Salmon

The first recorded domestication of Atlantic salmon in Norway was in 1969 (OECD, 2017). Currently Norway is the world leading producer of farmed Atlantic salmon, using some of the most advanced technology to provide good fish welfare as well as good quality fish.

Atlantic Salmon (*Salmo salar L.*) has an interesting life-history. It is a cold-blooded species in the family of Salmonidae, sub-family Salmoninae, genera *Salmo.* It is one of the most extensively studied species of fish in aquaculture. It is mainly found in the North Atlantic Ocean or in rivers that feed to the Atlantic Ocean. In Norway, farmed salmon will mature in the pens along the coast in sea water with an average size ranging from 4kg to 6kg (Norway, accessed 2018).

Atlantic salmon is a nutritious oily fish species. Per 100g of fish, the average content of protein is 20g, marine omega-3 fatty acids at 4.8g, Selenium at 30µg Vitamin B12 at 3.5µg and Vitamin A at 26RAE, that is used to provide immune responses, foetal development, improve reproductive capacity as well as provide good vision (Sea food from Norway, accessed 2018).

For good fish health and better quality of salmon, there are certain requirements that must be met. Atlantic salmon requires good water quality especially for its health in the early stages of development. Important water quality parameters include oxygen saturation, salinity, temperature, carbon dioxide concentration and microbial contamination. These indicators are regularly checked and recorded. The designs in modern aquaculture facilities allow for free and steady flow of fresh water in the pens.

Salmon require a constant supply of oxygen as a shortage can result in the death of many fish within minutes. Oxygen saturation can be maintained naturally by the constant flow of water or oxygen pumps are used to aerate the water. This is a backup plan that is recommended to sites that nurtures as well as protects the salmons needs in case of any mishaps (initiative, accessed 2018). Artificial photoperiods and ample temperature between 8-14$^{o}$C are utilized especially for offseason smolt production (Fjelldal, et al., 2006).

Sea water constitutes of 96.5% water, 2.5% salts and the rest are a combination of other organic and inorganic dissolved materials, some atmospheric gases and particulates. Atlantic salmon has phenotypic pliability which allows it to survive both in fresh water as well as salty sea

water (Klemsten, et al., 2003). In Norway, the need to genetically improve salmon has been systemic and in over 40years, farmed salmon has become better adapted to the commercial farming environment. The breeding programmes are family-based and are part of the most advanced programmes in international aquaculture. The effect of such breeding programmes has improved growth and reduced production cost (Gjerde, et al., 2007).

### 2.1.1 Atlantic salmon lifecycle

Production of farmed salmon is an all year-round process that takes place in batches. The complete lifecycle of Atlantic salmon is shown in Figure 2.1.1.

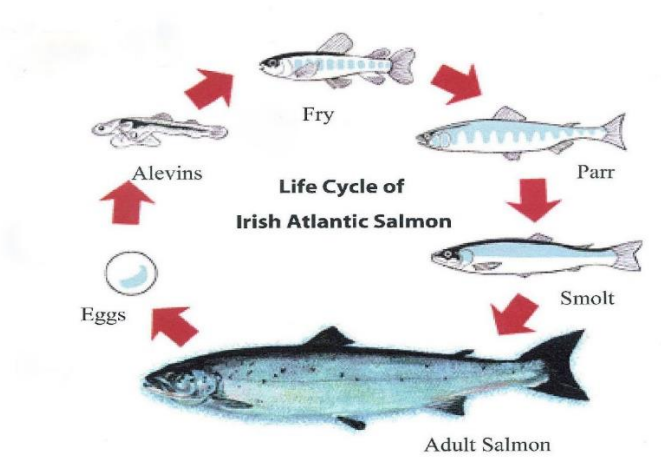


Figure 2.1.1 Lifecycle of Atlantic salmon (Marine Institute, 2019).

Roe from the female fish and milt from the male fish is taken and fertilisation takes place in freshwater as it would have in wild salmon.

Figure 2.1.2: Fertilised ova of Atlantic salmon (Marine Institute, 2019).

The temperature of the water determines the growth and development of the ova. After fertilisation, the ova are kept at the optimum constant temperature for eighty days. The eyes can be seen by the naked eye on the orange coloured ova when they are, on average, the size of a pea. The ova feed on the yolk sack and some activity can be seen during this time. If the ova turn cloudy or white, the salmon is dead, and they can be handpicked from the batch to avoid contaminating the healthy ova as they decay. Although there is a 95% survival rate in farmed salmon, there is need to have high fecundity to increase the odds. This also increases the selection intensity leading to a relatively high genetic gain per generation in breeding (Skaarud A, 2003).

The just-hatched fish are called alevins and still have the yolk sac attached to their bodies by spring. When their yolk sac is absorbed after about 6weeks, the alevins become increasingly active and can then be transferred to bigger tanks. The alevins fill their swim bladder by going to the surface of the tanks and taking a big gulp of air. This allows them to be buoyant and it is easier for them to swim around or hold their positions.

Figure 2.1.3: Freshly hatched salmon known as alevins (Marine Institute, 2019).

Salmon are referred to as fry when they can swim freely on their own. The fry in the wild would normally feed on microscopic invertebrates such as zooplankton, but in farmed salmon, fry can start being fed on pellets. Because of their small size, the pellets are less than half a millilitre in size. The salmon start to experience rapid growth and grow from 0.2g to about 3g in a short time. It is important to nurture the fry by maintaining the temperature of the water and oxygen availability. The fry continues to have the pellet size increased as they grow so they have enough nutrients required for growth in the feed.

Parr are kept in bigger and separate tanks where it is easier to control environmental conditions. Separate tanks also avoid cross contamination from different batches of fish. When parr attains a certain weight, usually between 60g and 100g, they can adapt in saltwater. This process of adaptation is known as smoltification.

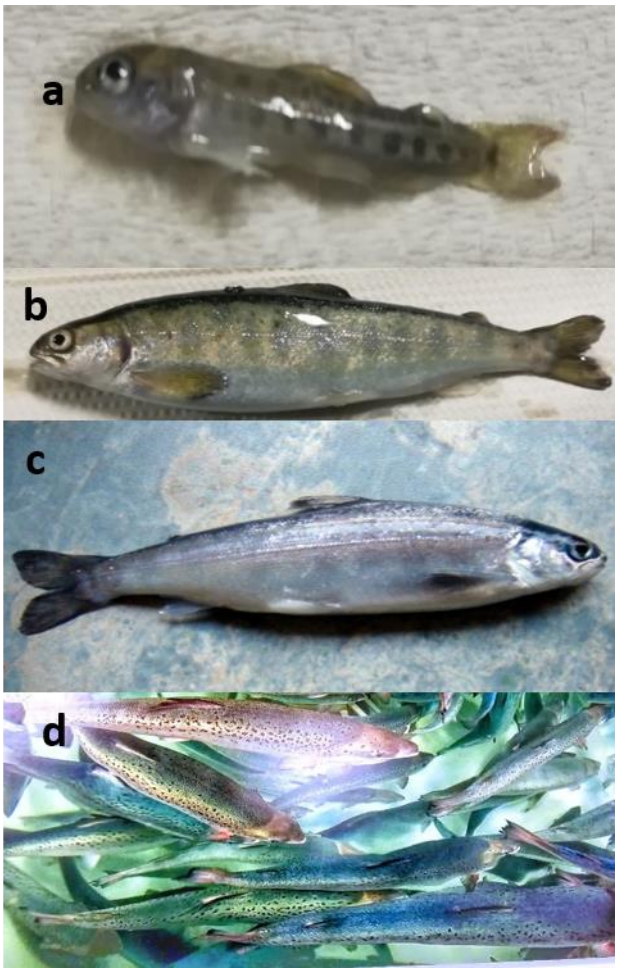


Figure 2.1.4: Development of Atlantic salmon during the freshwater stage: a) parr (own photo), b) before smoltification (own photo), c) smolt (photo Marine Research Institute), and d) adult salmon in seawater (own photo).

In the wild, the growth rate is essential to survival as larger fish are not targeted by other predators. In farmed salmon however, there is a normal distribution seen in the fish per tank. All the smolts will be fed the same pellet size of 4mm. In the beginning, the salmon is kept in fresh continuous running water under ordinary conditions. This means that there is continuous lighting from start feeding and the temperature was kept between 10$^{o}$C and 12$^{o}$C. During the process of smoltification, the photoperiod is often changed to 6 hours of light and 18 hours of darkness and the temperature can be lowered to 4$^{o}$C for about 6weeks (Kongtorp, et al., 2006).

Smoltification is then induced by exposing the parr to a square wave. The temperature is increased from 4ºC to 7ºC and finally to 10ºC. Fish are also being exposed to continuous constant lighting for 6 weeks before transfer to seawater is required. A saltwater challenge is done with a fraction of the fish taken into seawater with 35‰ for 24hrs. The process of smoltification is said to be complete when fish survive this challenge, and the shape of the fish starts to change, and the colour becomes a silver from brown (Johansson, et al., 2016). Most infectious diseases will become more pronounced post smoltification/ Sea Water Transfer SWT (Eggset, et al., 1999). These include the IPN caused by the infectious pancreatic necrosis virus and heart/skeletal muscle inflammation caused by the piscine orthoreovirus (Kongtorp et al., 2006).

When the process of smolting ends, the salmon are moved to larger tanks or the tanks in the sea. Here they will continue to be fed on pellets and grow. The adult Atlantic salmon can be identified by its streamlined body shape, shiny skin with black dots, dark blue upper-side and fat fin in front of the tail fin. Adult salmon can reach an average weight of 5kg in the 14-22 months they are kept in the seawater.

## 2.2 Quality

Quality can be defined as how the end-product fulfils the consumers expectations. The shape and colour of the whole body and fillets of Atlantic salmon are important sensory quality properties. An adult Atlantic salmon should have a streamlined body shape, shiny skin and bright moist eyes that are not sunken. The fish should have no vertebral malformations that alters the shape and may cause fillets to have cartilage and thus poor quality. Other important sensory quality properties are pink-red colour, firm texture of the fillets and pleasant sea smell. Nutritional quality, hygienic quality, technical quality are other quality categories that ensure consumer satisfaction (Skrede & Wold, 2008).

For the technical quality of Atlantic salmon, the suitability for processing is of high importance. For example, malformations of the vertebral column may result in decreased yield. Ethical quality has obtained increased attention recently and has a focus on sustainable production and animal welfare. Regarding animal welfare, normal development of the farmed salmon is considered of outmost importance. Hence, vertebra deformities and insufficient skeletal mineralisation are considered as problematic with regard to ethical quality.

## 2.3 Bone structure/ skeleton

The fish skeleton gives fish its basic shape, support for the soft tissue as well as provide protection of the internal organs. The back bone of the fish, also known as the vertebral column should be solid.

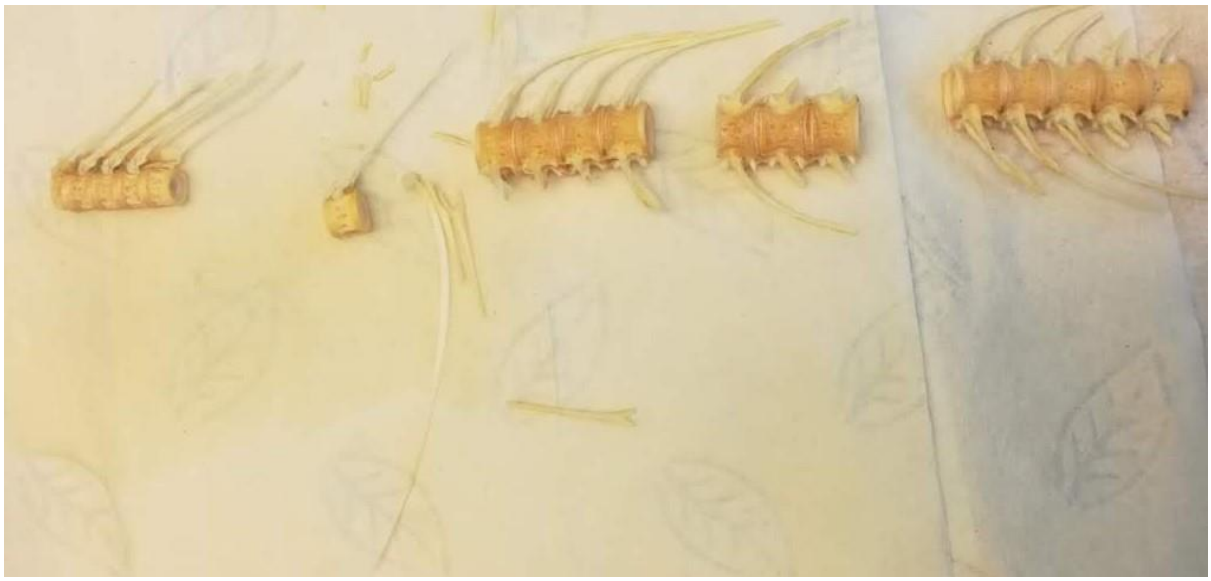

Figure 2.3.1 Fish vertebra and where rib bone connects viewed from the front (own photo).

The vertebral column is made up of a string of smaller bones known as vertebrae with a small hole in it (Figure 2.3.1). The small hole in the vertebrae makes a complete canal in which the spinal cord passes through. Thus, the vertebrae are also protecting the spinal code. In between the vertebrae, the space allows the vertebral column to move/bend resulting in fish motion as well as allowing nerves to reach tissue and other body organs (Earth, Accessed 2019).

Figure 2.3.2: Individual vertebra of Atlantic salmon (Exploring our fluid Earth, Accessed 2019).

Atlantic salmon has an average of 56- 60 vertebrae. The vertebrae can be described as a lightweight or flimsy structure adapted to a life in water. It has an hour glass shape and consists of four layers. These layers are made up of cells, minerals, proteins and fats as shown in the Figure 2.3.3 (Lall, 2002).

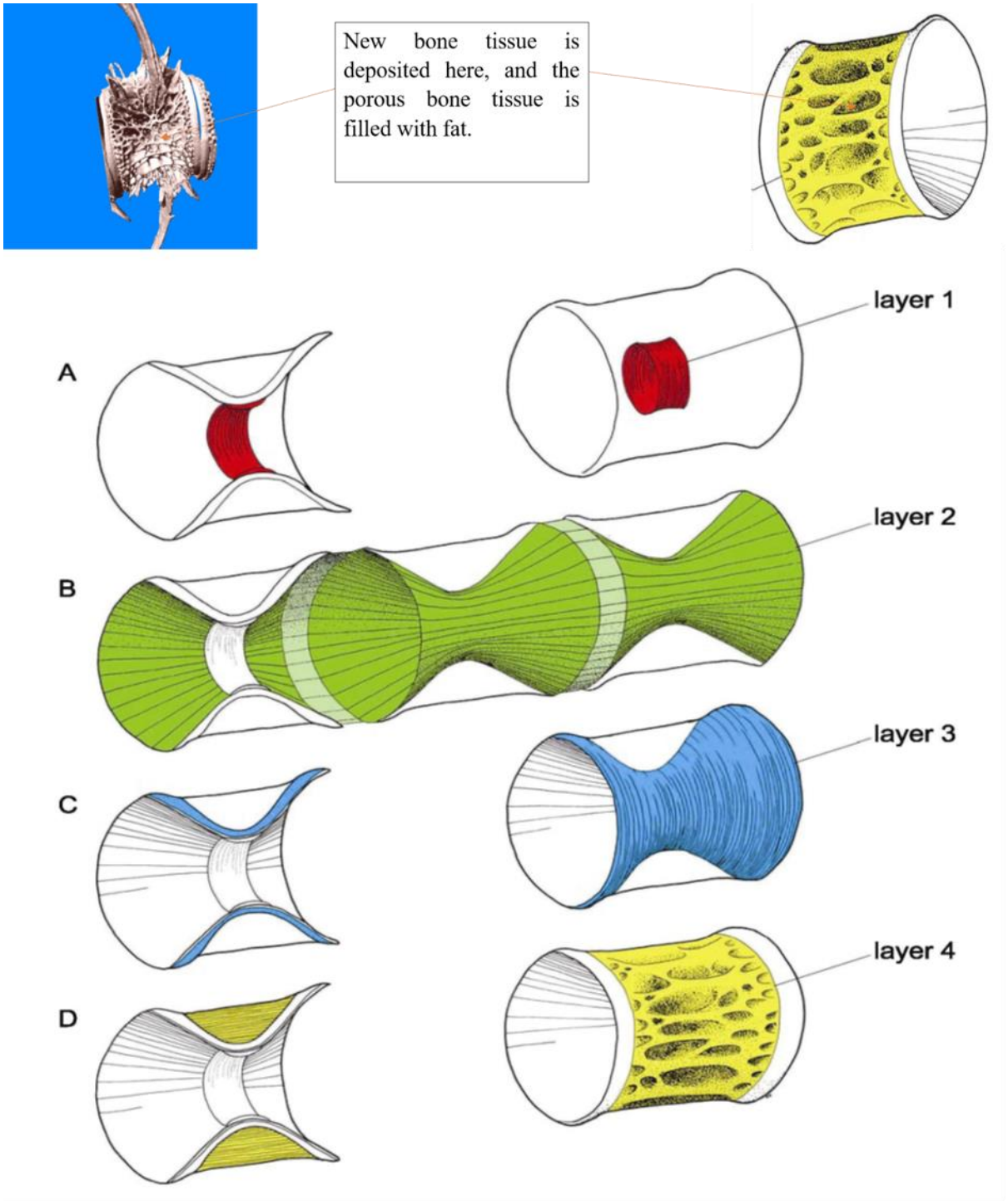


Figure 2.3.3: Position where bone is deposited on vertebrae (Hansen, 2019 pdf).

The protein of vertebra is mostly collagen and the minerals are mostly calcium from the water and diet as well as phosphorous from the diet. In the formation of vertebrae, proteins osteoid are deposited onto the bone surface and then mineralized - a process known as growth mineralization.

Calcium-phosphor hydroxyapatite salts are the main component in the inorganic part of the fish bones. They constitute about 65% of the bones dry mass and are fixed in type 1 collagen fibres (Moro, et al., 2000). These make about 90% of the organic part of the bone aiding in structural resistance and is the base for the biomechanical properties of the tissue (Mahamid, 2008).

The bone can be subdivided into the trabecular and the cortical bone. The trabecular bone is approximately eight times more active metabolically as compare to the cortical bone and is usually the first to show changes when response to a stimulus such as calcium deficiency. In the spine, the trabecular bone can be estimated to be between thirty and thirty-five percent of the total bone, thirty-five to fifty percent of the total bone in the distal radius and between sixty and seventy-five percent in the calcaneus.

The main anatomical regions of Atlantic salmon can be seen on the figure 2.3.4.

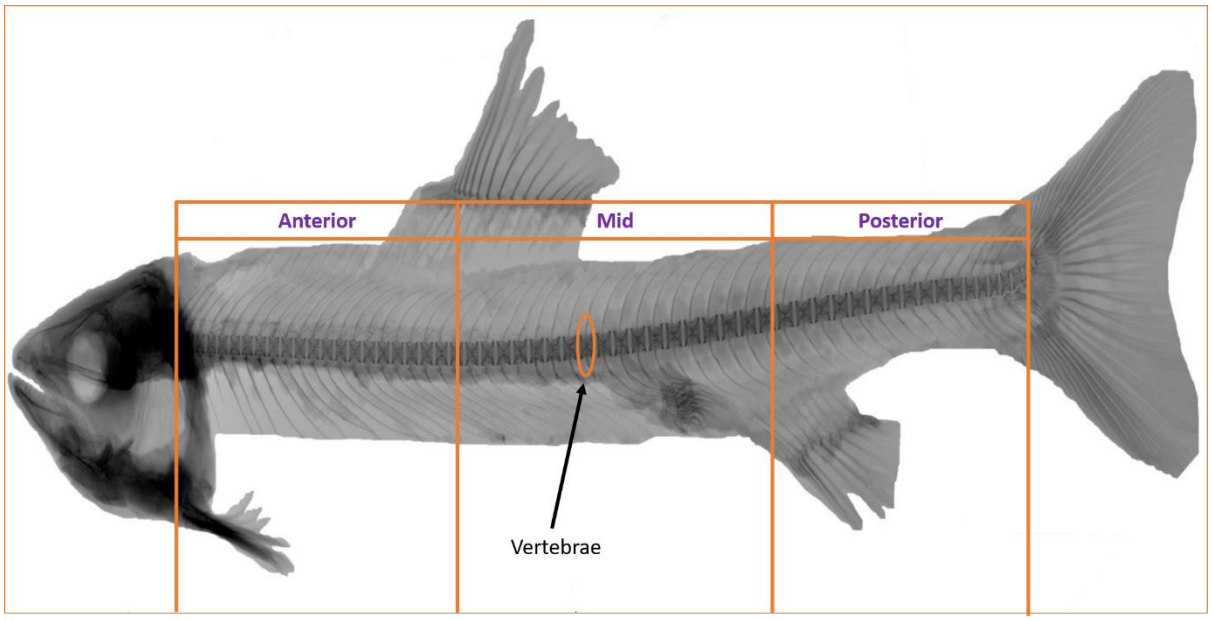


Figure 2.3.4 Image of Atlantic salmon skeleton showing the main regions and the vertebrae (Hansen, 2019 pdf).

The anterior end is the region close to the head end. It is characterised between the first vertebrae and the twentieth vertebrae. The mid is the region just under the dorsal fin to the start of the anal fin. It is from vertebrae twenty to vertebrae forty. The posterior end is the region that is from vertebrae forty to vertebrae number sixty.

## 2.4 Deformities

A major factor that contributes to the downgrading of many hatchery productions by about 7-20% of juveniles produced in marine institutes is the skeletal quality (Georgakopoulou, et al., 2010). Any deformities in the fish, though not well understood, will affect production costs, how the fish looks, its survival and ultimately its growth (Berillis, 2015). It is believed by some researchers that these deformities are induced during embryonic and post embryonic periods of life (Cobcroft & Battaglene, 2009), and are significantly affected by abiotic and nutritional factors (Georgakopoulou, et al., 2010; Sfakianakis, et al., 2006).

Deformities are a single or combination of different bone disorders usually associated with feed, environment or genetic factors (Fernández et al., 2008). Bone disorders or skeletal deformities are most common in the largest and strongest vertebrae. This is because there is more mechanical strain in these regions due to the fish movements when swimming and the composition of the bone is important in this flimsy structure. Most Atlantic salmon have a risk period of developing deformities. This can be in the early seawater phase /autumn smelting. As discussed earlier, the period of smoltification is a major physiological change characterized by rapid growth in fish and change in the vertebral column growth pattern.

Examples of deformities common in Atlantic salmon include vertebral malformations Lordosis, scoliosis, kyphosis, platyspondyly and vertebral fusion; jaw malformations bent, reduced lower jaw, harelip, front and downwards protuberance of jaw; spinal malformations compressed snout and neck bend; reduced or uneven fins, short jaw and deformity of the branchial arches (Berillis, 2015).

### 2.4.1 Vertebral fusion

Very few vertebrae can fuse without causing any significant or visible physical changes to the fish. However, if a lot of vertebra fuse, the result can be a shortened anterior/posterior vertebral column resulting in a fish with a hunch back or a short tail. At the point of fusion, there could develop nodal thickening as well (Witten, et al., 2005).

### 2.4.2 Compression

In autumn smelting, some of the smolts develop low mineral content. This in turn leads to a compressed vortex morphology. Swirl compression is highly evident between vertebra 31 and

49. This deformity can be curbed by ensuring the feed composition in the early water phase of these autumn smolts caters for their mineral requirements (Fjelldal, et al., 2006).

### 2.4.3 Jaw deformity

The fish can have a bent jaw, a reduced lower jaw, harelip or front and downwards protuberance of the jaw.

Other deformities include reduced or uneven fins, short jaw, deformity of the branchial arches, adhesions, curvatures, lordosis, scoliosis, kyphosis and platyspondyly.

## 2.5 Causes of deformities

### 2.5.1 General Breeding

The genome is a total of all genes on all chromosomes. Investigations into the structure and function of many genes in a simultaneous fashion is referred to as genomics. This study has many expectations including in new approaches in aquaculture. Application of genetics in aquaculture is a recent development (Balon, 1995b). Although genetic improvement is advancing in aquaculture, there is still indistinguishable differences between the wild and the farmed fishes (Eknath et al., 1991).

Usually, the traits selected for breeding programmes have an economic contribution to the producer. It is important to keep in mind that traits that have additive genetic variance can be improved and are the ones considered in breeding programmes (Douglas, 1986). In recent years, Marker Associated Selection has been employed to select for specific gene loci when the proportion of the additive genetic variance that is related to a locus/loci is greater than the heritability of the trait (Ferguson & Danzmann, 1995).

Micro-satellites probes are being used to show the high levels of genetic variation. They are also used to help in the identification of useful loci enabling the establishment of pedigrees in mixed family groups. Apart from the common advantages of being able to rear fish in a single facility and the ease in genetic analysis from fin clips, genetic analysts can use this as a way of determining what family to continue breeding as is or what family to improve on its breeding goals (Herbinger et al., 1995).

In animal breeding, it is important that the trait that is selected for is heritable. This means that the individual organisms distinguishing feature or characteristic can be passed on by the genes

inherited from the parent. The selection in animal breeding is made possible if the individuals have different genetic backgrounds. This allows advantageous individuals to be selected for and the less advantageous individuals to be selected against. These individuals selected will determine the next generation if allowed to mate. In animal breeding, a deviation from the populations phenotypic average from one generation to the other, will allow the breeder to record a success or otherwise. This means that breeding is measured at population level per generation and recorded as genetic gain (Oldenbroek & Waaij, 2014).

In animal breeding, the traits of an animal are reflected on its offspring and there is need to have a good quality stock of fish that is to be consumed by the public. Slaughter quality traits bred for include good quality fillets with no deformities or cartilage. Deformities or cartilage in the fillets can result from skeletal deformity.

A high rate of inbreeding in a fish breeding programme will result in a short-lived genetic gain. Other consequences of inbreeding include inbreeding depression, genetic drift and expression of deleterious recessive genes. In fish breeding programmes, there are three ways to control inbreeding:

1) Changing the breeding scheme restricting the number of families and candidates per family that are selected for breeding. However, all recorded fish can be breeding candidates.
2) Restriction of selected individuals per family for example, selecting less than 8 individuals per family.
3) Make use of the Optimal Contribution procedures. This however, cannot be used efficiently in fish breeding schemes due to the sheer number of fishes per family (Meuwissen T, 1997).

In aquaculture, part of the full-sibs are taken for checking traits like disease resistance and therefore they are not available for selection and no records are available for the actual full sibs available for selection.

### 2.5.2 Genetic effect on skeleton

The genetic effect involves mutations of the genes. A study done in 1996, isolation of 109 mutations that disrupt pharyngeal arch development in zebrafish was done. Of these, the posterior arch, the hyoid and five branchial segments supporting the gills were mainly affected by 59 of the mutations (Schilling et al., 1996). In zebrafish, mutations in the sucker gene, schemerle gene, hoover gene, sturgeon gene and gaping mouth gene results in a reduction in frontal arch elements.

However, the posterior arches are less likely to be affected (Piotrowski et al., 1996). A dominant mutation called the chihuahua was isolated. This mutation affects bone growth, after mapping and molecular characterization. The defect was seen to be in the gene encoding the collagen Iα1 chain. A similarity of the collagen assembly process and the importance of the type I collagen in bone formation was seen through the chi molecular characterization (Fisher, et al., 2003).

### 2.5.3 Environmental effect on skeleton

#### 2.5.3.1 Heavy Metals

Literature suggests that skeletal deformities can result through the environment in two ways. The first is neuromuscular effect. Column deformities may be observed without any change in the chemical composition of the bone (Divanach et al., 1996). These deformities are mainly in the cranial, medial and caudal part of the vertebral column and can be attributed to the bacteria Flavobacterium psychrophilum (Madsen & Dalsgaard, 1999). Another probable cause of such deformities can be attributed to heavy metals such as Lead (Pb). Pb can be found in many industrial effluents. It is a highly toxic element and can impair development and bone formation (Davies, et al., 1976).

Cadmium (Cd) is also believed to contribute to vertebral anomalies in fish. Continuous exposure to Cd results in abnormal bone metabolism, calcium loss thereby weakening the bone, shortening and assimilation of cartilage. Vertebral curvature results from the spinal column being used as a fulcrum through the action of the caudal musculature. For Cd to affect the vertebrae, the calcium to phosphorous ratio due to loss of calcium will be low (Muramoto, 1981).

Other toxic elements or metals that may cause skeletal malformations include zinc, where larvae from eggs exposed to zinc were significantly shorter than controls with eye malformations, jaw deformities and branchial arches (Somasundaram, et al., 1984). C-shaped tails curved downwards and restricted caudal fin movement was observed in mercury contaminated water (Heisinger & Green, 1975). Spinal flexures were reported to be a result of exposure to mercury (Devlin, 2006). Spinal malformations, head enlargement are examples of findings in larvae exposed to copper as embryos (Sarnowski, 1998).

The second is in changing the biological processes essential in maintaining the bone biochemical integrity (Divanach et al., 1996). Again, there is a possibility of the effect of

parasites on the deformities seen. An example associated with the destruction of cartilaginous tissue by *Myxobolus elliposoide* spores causing lordosis and compression of the caudal region (Bucke & Andrews, 1985).

#### 2.4.4.3.2 Dissolved oxygen concentration

The term dissolved oxygen is used to describe the amount of free, non-compound oxygen in any fluid. The oxygen molecules are not bonded to any other molecule. The oxygen molecules bonded to other molecules do not contribute to the dissolved oxygen concentration. The amount of dissolved oxygen determines the livelihood of aquatic life. A level that is too low or too high can cause detrimental effects. Fish get oxygen into their bodies through their gills for respiration. The dissolved oxygen in the water comes from both the air and the plant life in the water.

### 2.5.1 Water Temperature

An experiment was carried out in *Sparus aurata* during the autotrophic and exotrophic larval periods to determine the effect of temperature on the development of the inside folded gill-cover. At 16ºC, haemal lordosis was observed. This was fluctuating response against the temperature. Mild deformities of the caudal part was also observed when 16ºC was used in the exotrophic larval stage. Deformities of the dorsal fin were observed when 22ºC was used during autotrophic and exotrophic stages (Georgakopoulou et al., 2010). For Atlantic salmon, recommendations limiting temperatures to safe levels, ≤8°C during egg rearing and ≤12°C after fist feeding, led to substantial reductions in skeletal malformations (Baeverfjord, 1999).

### 2.5.2 Velocity of water current

The skeletal malformations are greatly influenced by the water currents. Previous experiments suggest that 21-25% of juvenile sea breams developed lordosis when they in water with velocity of 10cm/s (Kihara, et al., 2002).

### 2.5.3 Tank Colour

The colour of the tank was seen to influence jaw malformations in larval striped trumpeter *Latris lineata.* It was seen that 44 days post-hatching, malformed jaws were observed in red tanks, followed by green, white, blue, black and lastly marble (Cobcroft & Battaglene, 2009).

### 2.5.4 Nutritional factors

Phosphorous deficiency is known to cause abnormalities in the skeleton. Haddock juveniles fed on a 0.42% phosphorous diet had curvature of the vertebrae close to the caudal region. The spine and lower part of the vertebrae also showed deformities in the case of a deficiency in phosphorous. It is also important to note that excess phosphorous in the diet causes excessive excretion into the environment and affects bone mineralization (Roy & Lall, 2003). Post-smolt rapidly growing Atlantic salmon show soft bones and skeletal deformities in phosphorous deficiency (Baeverfjord, et al., 1998).

Vitamin C deficiency can be identified from cases of kyphosis, scoliosis and lordosis. Skeletal abnormalities to the cranial, medial and caudal region of the vertebral column in rainbow trout fed low Vitamin C concentration diet were observed (Dalsgaard & Madsen, 1999). The Vitamin C deficiency is dependent on the fish species. In cases of the malformations caused by this deficiency, it is because either the fish cannot make its own vitamin C or the amount of vitamin C produced does not allow for the normal formation of bone, connective tissue and cartilage in the fish itself (Lim & Lowell, 1978).

Vitamin A in high concentrations have resulted in vertebral deformities in gilthead sea bream juveniles. This is through advanced bone mineralization, resulting in higher mechanical load at vertebral endplates and the fish' downstream bone remodelling process (Fernández, et al., 2012). Hypervitaminosis A quickens the vertebral column precocious mineralization. This may result in deformities like curvatures, compression, fusion and jaw deformities (Dedi, et al., 1997; Haga, et al., 2003; Takeuchi, et al., 1998).

Vitamin K is necessary in regulating bone formation through osteocalcin synthesis by the osteoblasts. This is very important in bone mineralization and structure. A decrease in Vitamin K in haddock showed a decrease in bone mineralization, lower bone mass and more pronounced bone deformities (Roy & Lall, 2007).

Vitamin E is responsible for the antioxidant protection of the cell membranes. Skeletal muscle degeneration is a side effect of the deficiency of Vitamin E in addition to increased mortality (Fjelldal, et al., 2006).

### 2.5.5 Abnormal swim bladder

An oily surface of the tanks may cause abnormal swim bladders. In the absence of a functional swim bladder, it was observed that juvenile red sea breams had difficulties staying at the surface or in the water column. They adopted an aberrant swimming style of slanted, nervous and jerky movements. This increased the incidence of lordosis as the axial skeleton gradually deformed. Curvatures were identified in the region with highest muscle pressure during swimming. Inflation of swim bladder at later stages of fish development do not reduce the curvatures of fish with chronic lordosis from larval stages (Chatain, 1994).

### 2.5.6 Other Factors

Skeletal damage may be caused by electrical shock used in electrofishing. A study with 209 captured adult rainbow trout, 50% of them showed spinal injuries with an average of 8 vertebrae dislocated and/or splintered. It was shown that radiation- quarter sine waves injured more vertebrae per fish as compared to exponential pulses or square wave pulses (Sharber & Carothers, 1988).

Another factor contributing to skeletal deformities is the exposure of Atlantic salmon to non-lethal but damaging amounts of radiation. Radioactive and non-radioactive isotopes are commonly indistinguishable from each other because the chemical behaviours are like each other (Press, 1957).

Other cause of vertebral deformities can be linked to heaving of farmed salmon during weight sampling or reduction of biomass. Parr are small and can easily be harmed by this process thus it could be a factor to keep in mind during handling of fish. Brood stock condition and egg quality coupled with extreme environmental conditions may be a causative factor as well to skeletal malformations.

## 2.6 Radiography

This is the use of X-rays in the analysis of the fish skeleton. Object size and a weak contrast affect the reliability of the x-ray results. Weak contrast comes from the level of mineralization in the bone. It is ideal to diagnose any malformations early and thus very small fish may be sampled. An example is in a developing fish that has a fork length of 8cm, the vertebrae would be less than 1mm with very low mineral content. It is thus difficult to produce a clear image with good contrast. It is important to note that this level of mineralisation varies between

species. Thus, a diagnosis can be done on a sample of similar size to another sample that produces no viable results for diagnosis.

Calibration of radiography equipment requires a skilled radiography technician. The three main settings that should be well-adjusted for the finest results are:

1. Kilovolt kV that describes the voltage used in the imaging
2. Milliamp x seconds mAs- This describes the electron current against the positively charged electrode anode multiplied by the exposure time in seconds.
3. Film-focus distance- This can be fixed in mammography or adjusted within a wide range in a standard radiography setup.

The radiation dosage is a combination of the first two settings kV and mAs. Universal guidelines in relation to this is uncommon because different equipment have different setting and the results are highly variable. There are general considerations that can be employed as guidelines in imaging using radiography. These are:

1. Lower radiation doses are required in fish as compared to their counterparts to produce an image.
2. Improvement of the quality of the image can be done through increasing the mAs.
3. Decrease in the contrast of the image greyer image when kV is increased.
4. Increased kV results in a better penetration and this can be an advantage when sampling thicker objects.
5. Darker images are a result of increased kV and mAs.
6. A larger exposure area can be created by increasing the film-focus distance but fewer x-rays reach the film in this way as they spread indirectly from the source. This reduced the quality of the image.
7. A film covered by a silver salt emulsion is exposed to x-rays and the film is developed to produce a standard radiography image.

Advantages of radiography include

1. Diagnosis of malformations in the skeleton can be done without opening the fish.
2. It is simple to perform.
3. It takes a short time to perform the whole procedure.

Disadvantages of x-ray

1. Cannot penetrate bone and other hard substances but only soft tissue
2. In digital radiography, the image is made up of pixels and fine details cannot be seen clearly.
3. Low contrast of soft tissue structures due to superposition of bone
4. Loss of detail in images from analogue radiography during development of images. The image is on a film-foil that was exposed to x-rays, thus a picture or scan must be done to make the image digital.

### 2.6.1 Computed Tomography (CT)

Computed Tomography CT was first introduced in 1971 in axial imaging of the brain in neuroradiology. It was further adapted for three dimensional 3D whole body imaging. Currently, CT is used in diagnosis and follow up studies of target individuals as well as in the screening of healthy subpopulations with specific risk factors such as vertebral column malformations otherwise referred to as deformities.

CT estimates the yield of slaughter quality traits by making use of 3D image analysis of the X-ray absorption properties. This stems from the background that different tissues have different absorption properties. However, the final images obtained are more reliable and easier to handle when they are two-dimensional 2D axial or reformat black and white images. The contrast and resolution of the images highly influences how deformities are categorized. The quality of images is also influenced by the size of the specimen, the standardization of the CT scanner and preparation of samples.

DTI, with more than 10years of experience in image analysis and CT scanning produced a laterolateral view of the fish that were scanned. DTI has further developed an online CT scanner that can be placed in high demand production lines significantly reducing the cost of labour and materials for manual dissection as well as human error or operator dependence when performing manual dissections.

### 2.6.2 Principles of CT scanning

X-ray transmissions are measured through a specimen for many views. These different views are attained in three different ways. The first is through detectors that have between 800 and 900 detector elements along the detector arc.

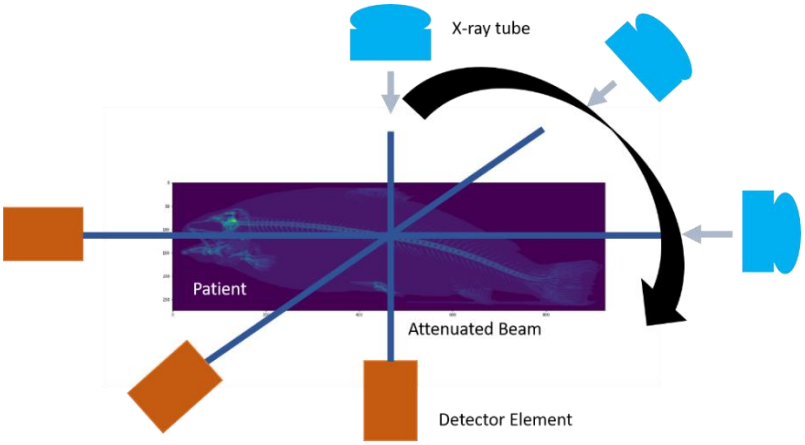


Figure 2.5.2.1 A series of measurements made at any point along a line by in effect rotating the x-ray tube and detector about that point.

The second way is by tens or hundreds of detector rows laid next to each other along the axial rotation. The last way is through rotation of the x-ray tube around the individual of interest taking as many as 1000 angular measurements.

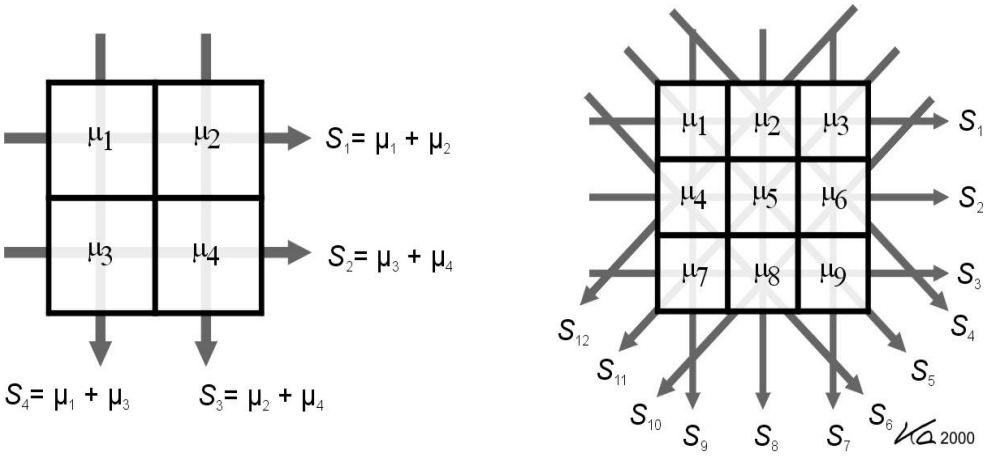


Figure 2.5.2.2 Attenuated x-ray beams as projected from rotation about the specimen.

The attenuated beam is transmitted through the specimen and meets different tissue which has different linear attenuation coefficients.

The beams from the x-ray tube are parallel to each other and come from many angles. This multiple projection ensures solving the issue of density ambiguity in an image.

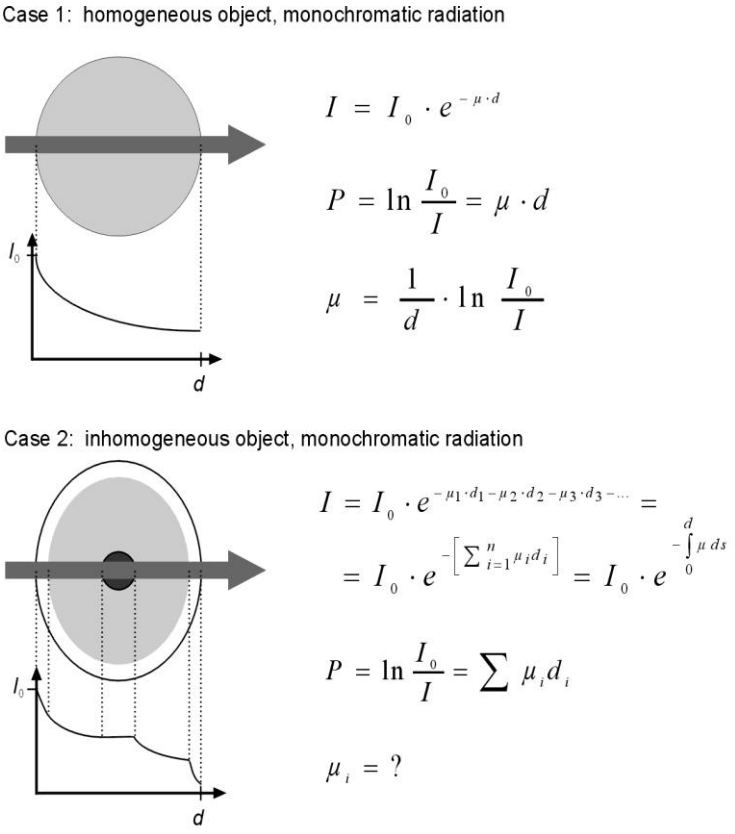


Figure 2.5.2.3 Linear attenuation coefficient of an attenuated x-ray beam passing through a homogeneous object Case 1 and an inhomogeneous object Case 2

Where

Id = intensity of the distance

$I_0$.e = the unattenuated X ray beam

$\mu_i$ = linear attenuation coefficient

x = thickness of the specimen

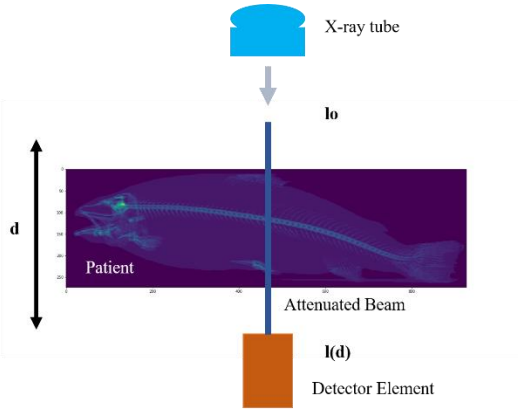


Figure 2.5.2.4 An attenuated x-ray beam passing through a specimen

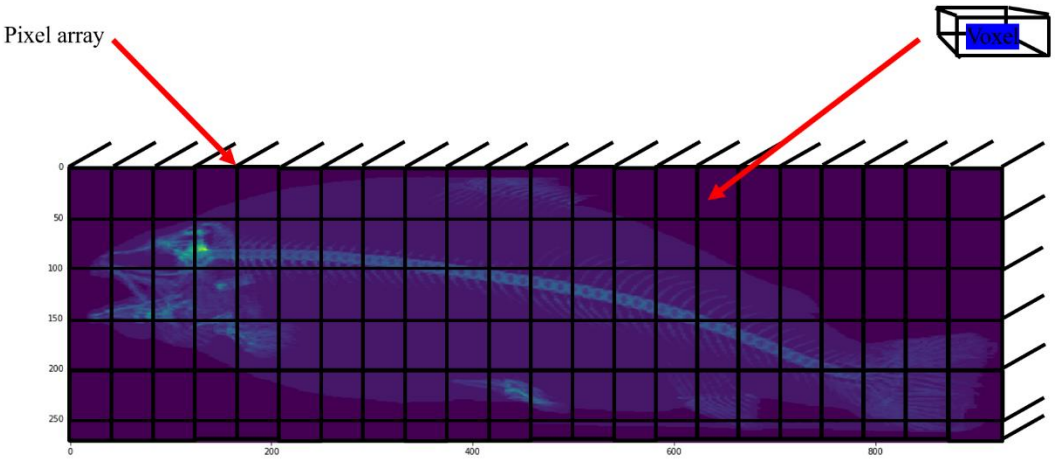


Figure 2.5.2.5Image showing the pixel and voxel of a CT scan image.

According to Beer's Law, only the primary beam is considered for attenuation and the remaining scattered x-ray beams are ignored. The image produced on the CT is made up of a matrix of picture elements or pixels points on the lines of x-ray attenuation when viewed on a display monitor that represents the mean linear attenuation coefficient in the voxels points on the lines of x-ray attenuation when kept in the computer for use in quantitative purposes, representing volume elements due to the finite thickness of the 'slice'. The voxels are the associated volume elements 3D and pixels are picture elements 2D.

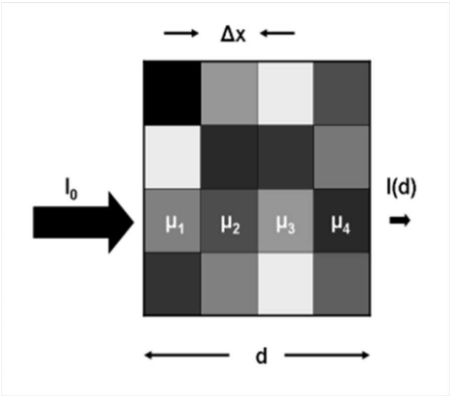


Figure 2.5.2.6 A 4 x 4 illustration matrix that shows the measurement of a transmission along one line.

In principle, each element in the matrix may have a different value of the associated coefficient. This means that CT images can be recorded from the basic measurement of the intensity of attenuated and unattenuated x-ray beams. The basis of the CT image is the matrix of linear attenuation coefficients used in image reconstruction. This attenuation can be expressed as

$$Id = I_0 e^{\wedge -\sum_{i=1}^{i=4} \mu i \ \Delta x}$$

Where

Id = intensity of the distance

$I_0 e$ = the unattenuated X ray beam

$\mu_i$ = linear attenuation coefficient

i= number of positions in the matrix

$\sum_{i=1}^{i=4} \mu i \ \Delta x$ = summation of the linear attenuation coefficient with respect to the thickness of the specimen measured.

2.6.3 CT image reconstruction

Waves are a result of movement of energy. X-rays are an example of such waves. They a very short and powerful waves that do not require any form of physical medium to be conducted. X-rays can also be known as radiation and cannot be seen by the naked eye. However, they can pass through different forms or objects with low densities like muscle. Bones have a higher density than the surrounding tissue thus a shadow is refracted by the x-rays when they

encounter the bone. In an image, the bones will appear darker and the surrounding muscle and organs will appear faded (Kalender, 2005).

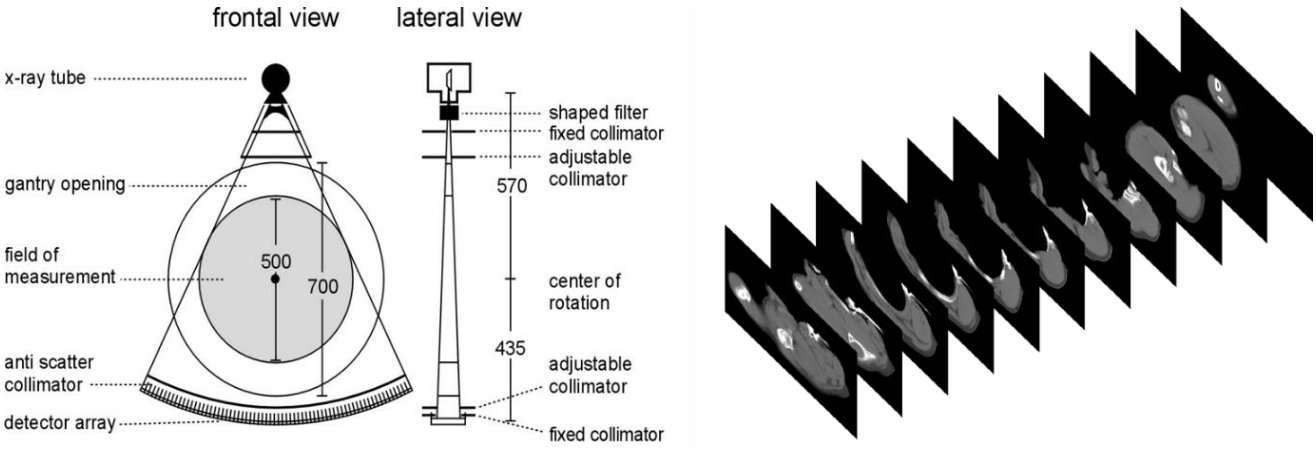


Figure 2.5.2.7 2D images produced about a point are stacked (Buzug, 2008).

In CT imaging, a combination of X-rays and computers is employed. This allows for a picture to be taken as well as viewing the internal parts of a specimen without physically opening the specimen. The images produced are cross sections with a three-dimensional dataset used in reconstruction of images. The two-dimensional images that are produced through a narrow x-ray beam circling a specimen at different angles may be stacked to produce a 3D image or any other plane (Buzug, 2008).

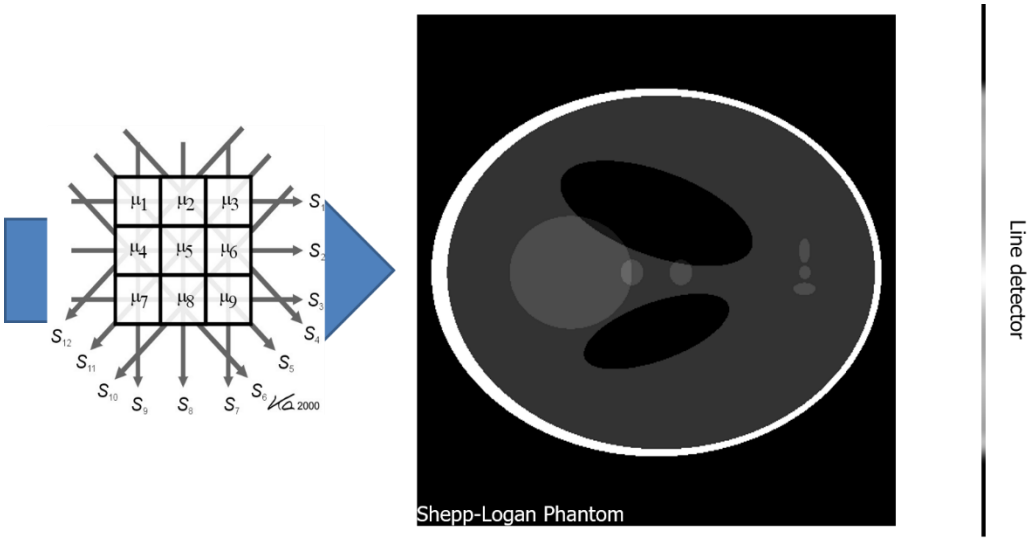


Figure 2.5.2.8 Image reconstruction through matrices

Projection reconstruction is a mathematical process used to separate the points along a line from one another and the lines that make up two-dimensional axial image planes. A map of the

x-ray attenuation coefficients in a cross-sectional slice of the specimen is produced and the density of the tissue at any point in the image can thus be determined. The number of points on a line and their size 0.25mm-1.5mm in any given CT scanner is variable as is the thickness of the slice 1mm-10mm. However, the size of a point or element in any reconstructed image is the same size and about 256-512 elements are along the line (Whitehouse & Adams, 1992).

Simple segmentation or other more advanced methods can be employed in image reconstruction and analysis. Through the use of faster computers and from analog to digital cameras, there is less fish handling. This has increased the efficiency and animal welfare during husbandry in the fish industry. Results can be recorded within a short time as milliseconds from when the specimen are put on the conveyer belt. When all the parameters are set to standard, the results can be trusted as they are more objective as compared to the alternative subjective visual screening (Hsieh, 2015).

Advantages of CT scans include

1. It takes less time to perform
2. It is painless
3. It is accurate
4. They can detect bone problems for example complex fractures
5. Non-invasive
6. Involves minimal radiation exposure
7. Provides morphological information
8. Provides information on tissue weakening
9. Accurately measures bone density
10. It is independent of size and provides a true volumetric density measure
11. More accurate than vertebral DXA
12. It is more simplified to use than other commercially available methods of measuring bone density
13. Improvement of high local contrast of soft tissue structures by CT

Disadvantages of CT scan

1. x-rays produce ionizing radiation which can cause cancer in a specimen or the person conducting the test by altering the DNA.
2. Window level which controls level of brightness that goes through and it is the midpoint of the range of CT number displayed. The lower the level, the brighter the image.
3. Interpretation of images requires skill and experience.
4. It is not yet an effective tool in measuring bone density
5. It is not readily available

## 2.7 Bone quality

The direct Hounsfield Unit can be used to measure the quality of a bone through its bone density. On its own, bone density is not a sufficient measure of bone quality unless the changes in the bone density are an indication of changes in the trabecular structure of the bone (Celenk & Celenk, 2008). Raw data from the CT is used in image reconstruction. The direct Hounsfield Unit can also be used to approximate density not only bone but also in tissue and muscle.

The HU is defined as the numerical unit assigned to each pixel in a computerized tomography CT image, according to its X-ray density. This is the linear transformation of the original linear change coefficient measurement. The amount of x-ray attenuation of each voxel in a 3D image is described using the HU. Voxel- in computer-based modelling or graphic simulation each of an array of elements of volume that constitute a notional three-dimensional space, especially each of an array of discrete elements into which a representation of a three-dimensional object is divided. Voxels are normally represented as 12-bit binary numbers and therefore have 212 = 4096 possible values (Kalender, 2005).

These values are arranged on a scale from -1024 HU to +3071 HU, calibrated so that -1024 HU is the attenuation produced by air and 0 HU is the attenuation produced by water. Using their radio densities, the fixed points on the scale are arbitrarily assigned as −1000 for air and 0 for water at standard temperature and pressure.

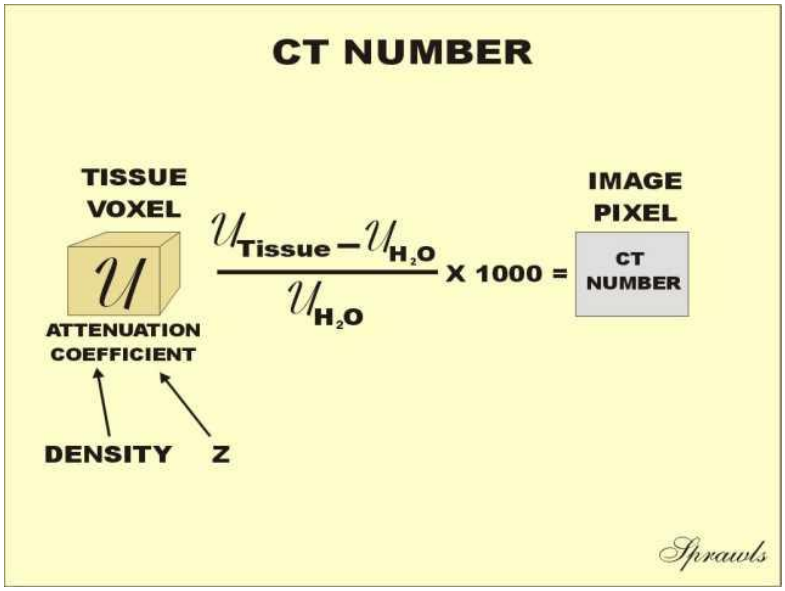


Figure 2.7 Image showing how the CT number is calculated (Sprawls Educational Foundation, Acessed 2019).

The CT image is viewed in a ‘window’. The range of Hounsfield units displayed window width and the centre point of the range of interest window level can be varied by the radiologist in order to observe specific tissues see windowing. The unit was named after Sir Godfrey Hounsfield 1919–2004, who developed CT scanning in the 1950s. Symbol: HU (Reference, accessed 2019).

### 2.7.1 Colorimetric characterization of bone

Bone densities otherwise known as bone mineral density is a clinical reference that aids in diagnosing risks of bone deformations or fractures. The amount of matter bone tissue per cubic centimetre a certain volume of the bone is used to determine this. The matter that is measured is calcium.

A reduced or low bone mass coupled with a high incidence in fracture can be a diagnosis of severe malformations in the vertebral column. Apart from this, the factors contributing to malformations of the bone for example, the internal bone structure genetics and lifestyle factors environment are problematic in quantifying hence bone density can be used. The overall risk for malformation development in the bones is more than half in any given individual and is quantitatively attributed to low bone density (Reinbold et al., 1988). Bone mass measurement can be clinically indicated by individuals with vertebral abnormalities through diagnostic tools from bone density measurements (Christopher & Cann, 1989).

### 2.7.2 Bone density measurement

As bone density is the measurement of the amount of bone tissue in a defined volume of bone, there are ways commercially available of measuring it. All these methods involve passing a low-intensity beam of x-rays/gamma-rays through the individual. A radiation detector that is set up on the other side of the individual captures the remaining radiation thereby measuring the rays absorbed by the individual. It is important to note that the beam is absorbed by both the bone and the surrounding tissue and the different methods available measure these differently.

In quantitative Computed tomography, a 3D or cross-sectional picture of the bone is directly measured without the influence of the surrounding tissue. The numerical density measured of the bone, which is calculated from the image is compared to historical or empirical known databases of bone density.

Bone mineral density tests can be calculated by imagej or by techniques using SXA single Energy X-ray Absorptiometry, PDXA Peripheral Dual Energy X-ray Absorptiometry, RA Radiographic Absorptiometry, DPA Dual Photon Absorptiometry, MRI Magnetic Resonance Imaging, Laboratory tests, SPA Single Photon Absorptiometry, ultrasound and DEXA (Dual Energy X-ray Absorptiometry that produces T-scores and Z-scores. These do not have an acceptable reference standard, so it is not used in diagnostics (Summers, 2015).

Bone mineral densities can be measured by Single Energy QCT and Dual Energy QCT can be positively correlated with an insignificant deviation of measurements as shown in biological samples (Rosenthal, et al., 1989). SEQCT measurements of bone density is influenced by the amount of intraosseous fat in the bone. A calculation was done which showed that for every 10% rise in intraosseous fat, the true bone density is underestimated by a factor of 7mg/ml (Reinbold et al., 1986). DEQCT eliminates the effect of the fat in the marrow during scanning, hence it is more accurate and reliable. The downside of using DEQCT is that the radiation factor is high and reproducibility is decreased (Genant & Boyd, 1977).

### 2.7.3 Imagej

ImageJ is a very useful and resourceful tool. Firstly, a phantom scan for reference is required to help set parameters of brightness and contrast to known values of calcium concentration. It is important to note that when looking at an image, brightness and contrast can alter what one sees. The colouring algorithm will colour the pixels in the image respecting the values that they show. For example: a dark image will have pixels with low values that require brightening for better visualization. This will alter the images values and the colouring also, because the algorithm will read the image and apply different colours to specific range values.

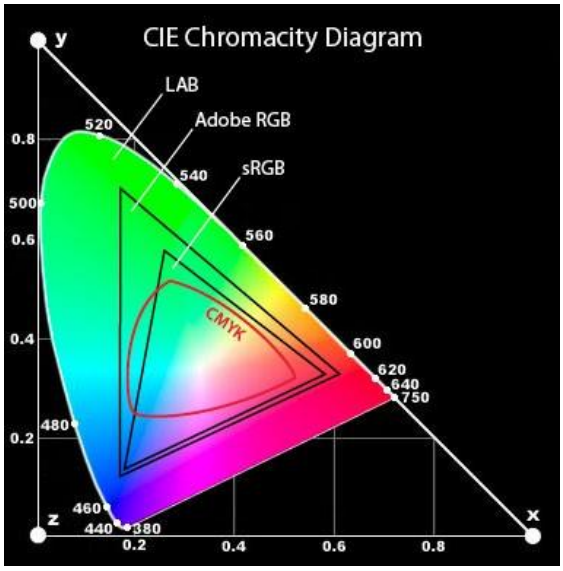


Figure 2.7.3.1 Cie-lab representation of colorimetric values as shown by different colour depicting tools (CIE, 1976).

In this study, Brightness, Hue and Saturation where kept at their original values. The freehand selection tool can be used to select approximately three to five vertebra per marked position and the Red, Green, Blue measure done. These give values in a different colour space hence transformation into Cie-lab, a colour space that humans see is required. Richard Hunter came up with a tri-stimulus L* a* b* model in the 1940's. This allowed for plotting absolute coordinates of colour and their differences. L* is for lightness 0=total absorption or blackness, 50=greyness, 100=total refraction or white; a* is for the Red/Green value on the x-axis, the more positive the a* value is, the more red the image is; b* is for the Blue/Yellow value on the y-axis, the more positive the b* value is, the more yellow and image is (X-Rite, 2019).

In Computed Tomography, the entire body of the fish is measured (Ciarelli et al., 1991; McB-room et al., 1985). The numbers that are generated, also known as x-ray attenuation of the tissue/ CT numbers or Hounsfield Units HU are used to quantify a property of interest in that region. The tissue measured is referenced to a known value that is indicated by a calibration standard. This is because the HU can be correlated to the density of biological tissue. As a result, the HU that is directly measured can be used as a reference for bone quality (Nilsson et al 1988, Shapurian et al 2006, Norton et al 2001).

In the trabecular zone of the bone, bone density is measured and used by the average HU within a region of interest ROI. As CT was one of the earliest methods used to measure bone density, it is referred to as the gold standard with which other measurements of bone density are

compared to Gugliemi et al 1994. Spiral acquisition, which is the development in CT technology and its software has made it possible to make use and apply this method in other areas and creation of 3D images.

The trabecular bone is approximately eight times more active metabolically as compare to the cortical bone and CT is the only method available commercially with the 3D technique. CT is thus a good method to use to measure isolated trabecular bone and the risk of malformations as it is highly sensitive to changes in the bone density (Reinbold et al. 1986).

On the ROI, a series of measurements are made at any point along that line by in effect rotating the source and detector about that point. It can perform without precise measurements or angulations and information is not wasted. The measurements of trabecular changes in the vertebral column takes seconds to perform. Value addition to routine BD measurements that can be done with the same CT data- no need for second tests (Gugliemi et al 1994). Actual bone density can be recorded in grams per cubic centimetre (Summers, 2015).

The x-rays used by CT scanners are kilovoltage meaning the photoelectric result and coherent scattering of the rays are of high importance. X-ray attenuation is not only highly dependent on the electron density but on the atomic composition as well of the region of interest. The CT number that is recorded is dependent on the geometrical configuration of the phantom system, the photon energy spectrum, the detector sensitivity as well as the reconstruction algorithm.

What is the connection between CT number and the effective density? The connection is such that the calibration of each CT system should be done for each scanning condition.

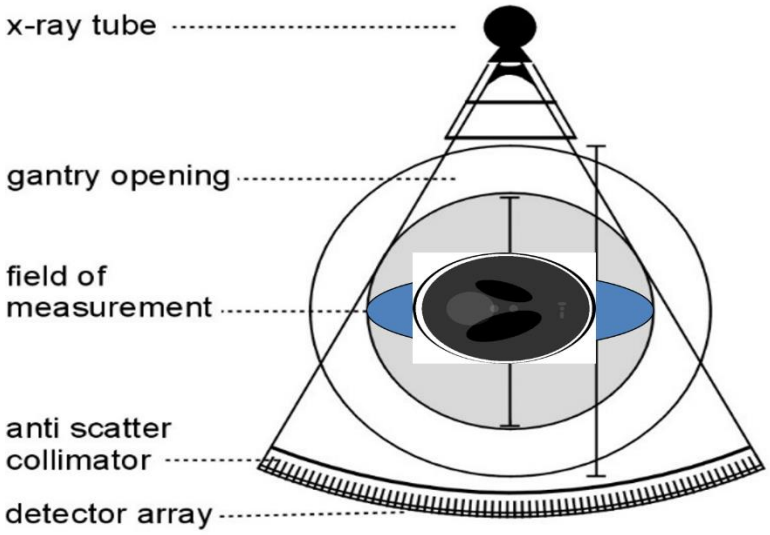


Figure 2.7.3.2 Illustration of CT scanning of a Shepp-logan phantom.

CT dataset calibration is required before the scanning is done. This is when a linear correlation between the density of measured region and HU is determined. The standard operating procedures entails the scan of a calibration phantom with already known densities. In this study, the Shepp-logan phantom was used.

It is important to note that there are various commercially available calibration designs that include both liquid and solid material that can be compared to bone. These different designs produce deviating scanning geometries. Scanner specific cross-calibration are then done to a standard reference using the region of interest data (Kak & Slaney, 1988).

This is done with reference to water, air and fat substitute ethanol (Brooks &Chiro 1976). The linear attenuation coefficient for the x-ray is directly linked to the CT number. The units provided allow for the approximation in quality of tissue by using the density measured. In this study, the technique used polybinary calibration gave a trabecular bone mineral density in $mg/cm^3$ as measured from a bone equivalent standard. The bone equivalent standard can be Calcium hydroxyapatite mineral or $K_2HPO_4$. The calibration also measured and produced HU for fat substitute ethanol. It is calibrated as follows: 0 units for water, -1000 units for air, -120 units for fat, +40 for muscle and +400 for bone.

The technique used in CT scanning is referred to as low-dose and uses radiation of 120kVp, 140mAs Rosenthal, 1989. The mean attenuation measure in HU of 5mm thickness is more

well-matched with any CT research. The term ROI refers t a manually defined tissue in every axial CT slice. If this is done, images can be enlarged without altering the results for accuracy.

## 2.8 Fish material for radiography

Freshly killed fish before onset of rigor mortis are most ideal in radiography. They must also be prepared for radiography by placing them sideways in a straight position. However, radiography can be done in live, dead, frozen or fixed fish as well. This is because in bone analysis, the deterioration of the bone is much slower compared to soft tissue.

### 2.8.1 Fixed samples

It is possible to stain bone and cartilage at the same time for radiography as adapted by Helland (2005) from Potthoff in 1984. Method of doing so:

1. Euthanize the fish.
2. Fix in 4% phosphate buffered formalin
3. Stain cartilage
4. Neutralize to avoid loss of calcium during bleaching
5. Bleach using bleaching solution. This step is optional.
6. Trypsin digestion using clearing solution.
7. Stain bone
8. Destaining
9. Preservation (Dingerkus & Uhler, 1977; Summers, 2015; Rosa-Molinar, et al., 1999; Gavaia, et al., 2000).

### 2.8.2 Frozen samples

If the fish are going to be x-rayed, they should be individually frozen on a tray. Fish smaller than 5g will defrost more quickly and are fragile even when well packed. On the other hand the weight of larger fish above 1kg present challenges in handling and storage. Trained and experienced technicians can fillet the large fish taking care not to cut into the spine. The spines should all be uniformly placed during imaging.

## 2.9 Heritability

Heritability is defined as the proportion of additive genetic variance to the total phenotypic variance and quantifies how large the fraction of phenotypic variance is due to variation in the breeding value.

$$\frac{\text{Additive genetic variance}}{\text{Total phenotypic variance}}$$

Heritability can be used to determine if the traits are sex determined or if the traits can be measured after death or on relatives. Low heritability is said to be less than 0.2. If there is a low heritability, there is need for further studies with more observations required. Selection in a family with low heritability will favour animals with positive environmental effect, limiting the response in the next generation therefore genetic effect is masked. Variation in the trait is said to be due to the environment residual variation or non-additive genetic effects fitness traits. Test stations are used to standardise the environment by reducing environmental variance.

Intermediate heritability is between 0.2 and 0.4 (Table 1). Most production traits will have this heritability when calculated. High heritability is said to be greater than 0.4. The differences are mainly due to difference in breeding values quantitative traits. If heritability is 1, the response to selection is directly proportional to the population average of selected individuals. Reduced heritability can be a result of reduced genetic variance. This is because the environmental variance is assumed to be unaffected by selection.

Table 1: Examples of heritability of some traits in Atlantic salmon and Rainbow trout: Animal species and trait heritability. (Oldenbroek & Waaij, 2015)

| Species Trait | Heritability |
|---|---|
| Survival | 0.05 |
| Body length | 0.10 |
| Body weight | 0.20 |

2.9.1 Estimating heritability

Heritability estimation can be done through various methods. The common rule in heritability

estimation is that there is need for assuming a large randomly effective mating population

size with no natural selection. This means there is no migration, selection, mutation, genetic drift. Methods developed consider the species to be diploid with normal meiosis and sex specific variances in recombination are included (Sakamoto, et al., 2000).

Regression between parents and offspring

This method estimated the level of transmission of a trait from a parent to the offspring

$$y= a + bx$$

Where x =mean value of the trait for the parent

y= mean value of the trait for the offspring

a= the intercept

b= the regression coefficient

The heritability is equal to the regression coefficient when the mean values of a trait used are derived from both parents.

$$\therefore h^2=b$$

On the other hand, if offspring are compared with only one parent, the heritability is estimated to be twice the regression coefficient.

$$\therefore h^2=2b$$

2.9.1.2Hierarchical Mating

In this method of estimating heritability, the source of the variation in the whole population is described.

$$Y_{ijk} = \mu + S_i + D_{ij} + e_{ijk}$$

Where $S_i$= Sire

$D_J$= Dam

k= Progeny

$Y_{ijk}$ = the measure of a trait on the $k^{th}$ progeny of the $j^{th}$ dam mated to the $i^{th}$ sire.

$\mu$ = the overall mean of the whole population

$S_i$= the effect of the $i^{th}$ sire

$D_{ij}$ = the effect of the $j^{th}$ dam mated to the $i^{th}$ sire

$e_{ijk}$ = the environmental plus genetic segregation effect on the $k^{th}$ progeny of the $j^{th}$ dam mated to the $i^{th}$ sire.

Heritability is estimated from:

- Sire component

$$h^2S = 4\left[\frac{\sigma^2 S}{\sigma 2S + \sigma 2D + \sigma 2e}\right]$$

- Dam component

$$h^2D = 4\left[\frac{\sigma^2 D}{\sigma 2S + \sigma 2D + \sigma 2e}\right]$$

- Sire + Dam component

$$[h^2S+D] = \frac{2\,\sigma 2S + \sigma 2D}{\sigma 2S + \sigma 2D + \sigma 2e}$$

Where $\sigma^2S$ = Sire component of variance

$\sigma^2D$ = Dam component of variance

$\sigma^2e$ = Environment + genetic segregation component of variance

In this method of estimation of heritability, it is important to note that the dam components of variance are very high because of the maternal effects, dominance and epistatic variance as compared to sire components of variance. This is especially important to note in cases where dams are nested with sires for example in fish where in vitro fertilization is more lucrative.

2.9.1.3 Factorial mating

In this method of heritability estimation, sires of one strain are mated with dams of one strain allowing for variance components partitions.

Table 2: Theoretical expectations of additive and non-additive effects

| Variance Component | $\sigma^2A$ | $\sigma^2 D$ | $\sigma^2AA$ | $\sigma^2AD$ | $\sigma^2 DD$ | $\sigma^2 Ec$ | $\sigma^2 EG$ | $\sigma^2M$ |
|---|---|---|---|---|---|---|---|---|
| Between Families | ½ | ¼ | ¼ | 1/8 | 1/16 | 1 | 0 | 1 |
| Within Families | ½ | ¾ | ¾ | 7/8 | 15/16 | 0 | 1 | 0 |

Where $\sigma^2_A$ = variance due to additive genetic effects

$\sigma^2_D$ = variance due to dominance;

$\sigma^2_{AA}$, $\sigma^2_{AD}$, $\sigma^2_{DD}$ = variance due to epistatic interactions of additive-additive, additive dominance, and dominance-dominance types respectively;

$\sigma^2_{Ec}$ = variance due to environmental effects between tanks;

$\sigma^2_{EG}$ =other environmental effects not due to tank effects;

$\sigma^2_M$ = variance due to maternal effects (McKay, 1986).

2.9.1.4 Use of breeding values

Breeding values have been predicted from large data sets in animal breeding and the selection criterion has been based on the Best Linear Unbiased Prediction BLUP of the additive genetic effects which require background knowledge of variance components. These variance components of mixed linear models in animal breeding have been estimated by restricted maximum likelihood (Hofer, 1998).

2.9.1.5 Inbred Lines

Heritability and genetic variance can be estimated using variance between and within inbred lines. $h_t^2 = \frac{h_0^2 (1-F_t)}{1-h^2F_t}$

Where $h^2_0$ = the heritability in the base population

$h^2_t$ = the heritability at time represented by generations t

$F_t$ = inbreeding coefficient at time represented by generations t

2.9.1.6 Linear estimates

Prospective parents are selected for which the estimates of the average phenotypic and genotypic values are from a population with a known and established pedigree. A line of regression is fitted through plotted points that stand for the population mean, phenotype and genotype on one axis and the selected parents mean, phenotype and genotype on the other. This straight line then determines the regression of genotypic on phenotypic values (Standards, 1969).

2.9.1.7 Discrete traits

Traits can be discretely projected onto binomial distributions for example Bone deformity versus no bone deformity. An underlying continuous scale can be used to estimate heritability quantifying the multiple gene effects (Robertson & Lerner, 1949).

2.9.1.8 Animal model

An animal model takes into account the individuals records into a single estimate of the breeding value of that individual. The pedigree information should be accurate and complete to be able to estimate heritability. The phenotype used in this study to speculate the presence of deformity in the vertebral column were recorded in the fillet. The phenotype is effectively the sum of genetic effects and residual effects.

2.9.2 Heritability can be further classified into:

1. Broad sense heritability is the proportion of the total variance that is directly resultant of genetic differences.

$$h^2 = \sigma^2_G/\sigma^2_P$$

where $\sigma^2_G$ =the genetic variance

$\sigma^2_P$ = the phenotypic variance

2. Narrow sense heritability is the fraction of the genetic variation that is resultant of genes with simple additive effect.

$$h^2 = \sigma^2_A/\sigma^2_P$$

Where $\sigma^2_A$ = the additive genetic variance

$\sigma^2_P$ = the phenotypic variance (Dempster & Lerner, 1950).

3. Realized heritability is then the total proportion of the response to selection to the selection differential. Because environmental conditions are highly dynamic between generations, estimates of the response to selection and selection differential are based on control populations (Verspoor, et al., 2008).

$$h^2 = R/S$$

Where R= the difference in average phenotype between the unselected and the progeny of the selected parents reared under similar conditions Response to selection

S= the difference in average phenotype between parents and the family selected from Selection Differential (Hard, et al., 2008).

### 2.9.3 Genetic correlation

This is an estimate of the shared additive genetic effect between two traits of interest.

# 3 Materials and Methods

## 3.1 Fish material

A resource population of Atlantic salmon (*Salmo salar* L.) with known pedigree from the breeding company SalmoBreed AS, Norway were used in the study: 100 full- and half-sib families, year class 2016, n = 1176 individuals. In the freshwater stage, each fish was individually tagged using PIT-tags that were injected into the buccal cavity. Subsequent to PIT-tagging, all fish were mixed and reared communally until slaughter. Analysis of the fish were carried out from the 6$^{th}$ of March to the 9$^{th}$ of March 2018.

## 3.2 CT scanning and image analysis

Whole body scans of the salmon were taken using a mobile medical CT scan equipment (Toshiba Aquilon mobile computed tomography (CT) system). The 400mm field view underwent 112 exposures at 150mA tube current and 100kV. From this, 16 slices of 2mm slice thickness with 0.781/0.781pixel size manually developed the image (Figure 3.1). Three fish were scanned at the same time.


Figure 3.1 (a) Fish set on prepared fixture ready for CT scanner and (b) Scanning of fish.

A scan of a calibration Shepp-logan phantom with already known densities was done to ensure standardisation of the protocol and determine that the CT scanner was working effectively.

Traceability solution and CT scan data management system was put in place. Test report on effect of PIT-tag RFID and other tags on CT scan was done. The quality control scan was done using the known standard of a phantom. Figure 3.2 shows the Shepp-logan phantom and illustrates the standard HU for different tissues. These correspond to the predetermined values of different tissue indicating the CT scanner was optimal and standardised.

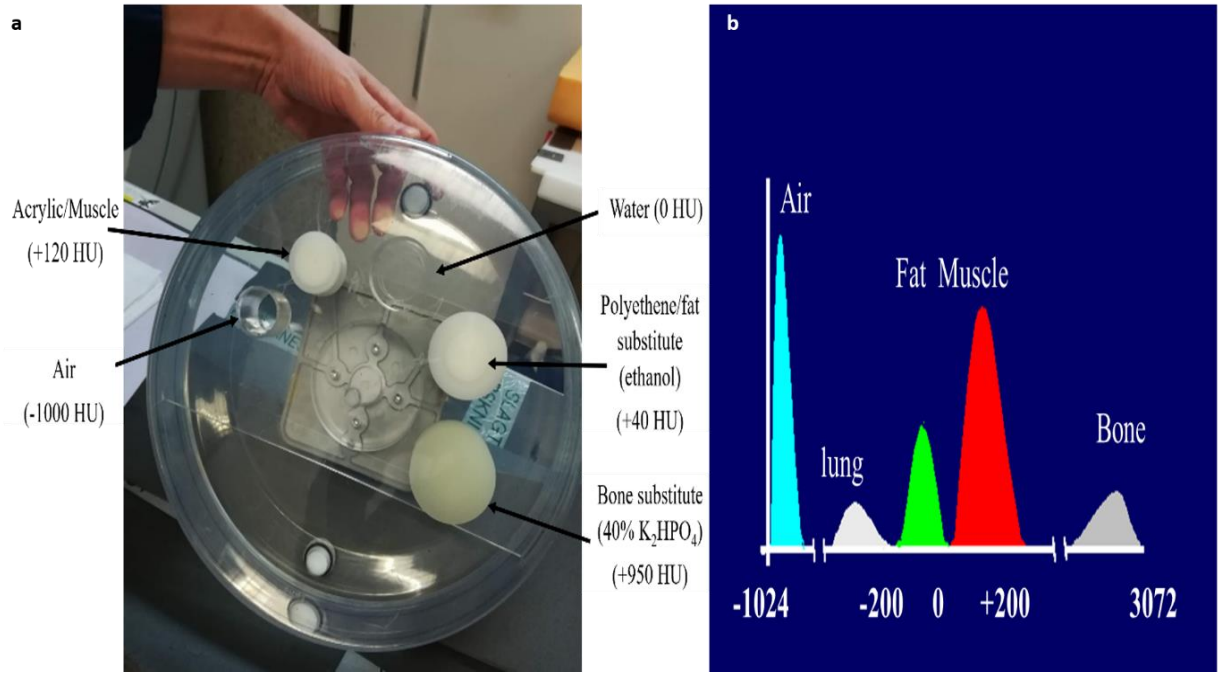


Figure 3.2: (a) Shepp-logan phantom scanned to calibrate the CT scanner and (b) Graph showing the HU of different tissue on a standard phantom.

Digitization of developed images was done and stripped of other slaughter quality traits to remain with the vertebral column using different software as shown in Figure 3.3.

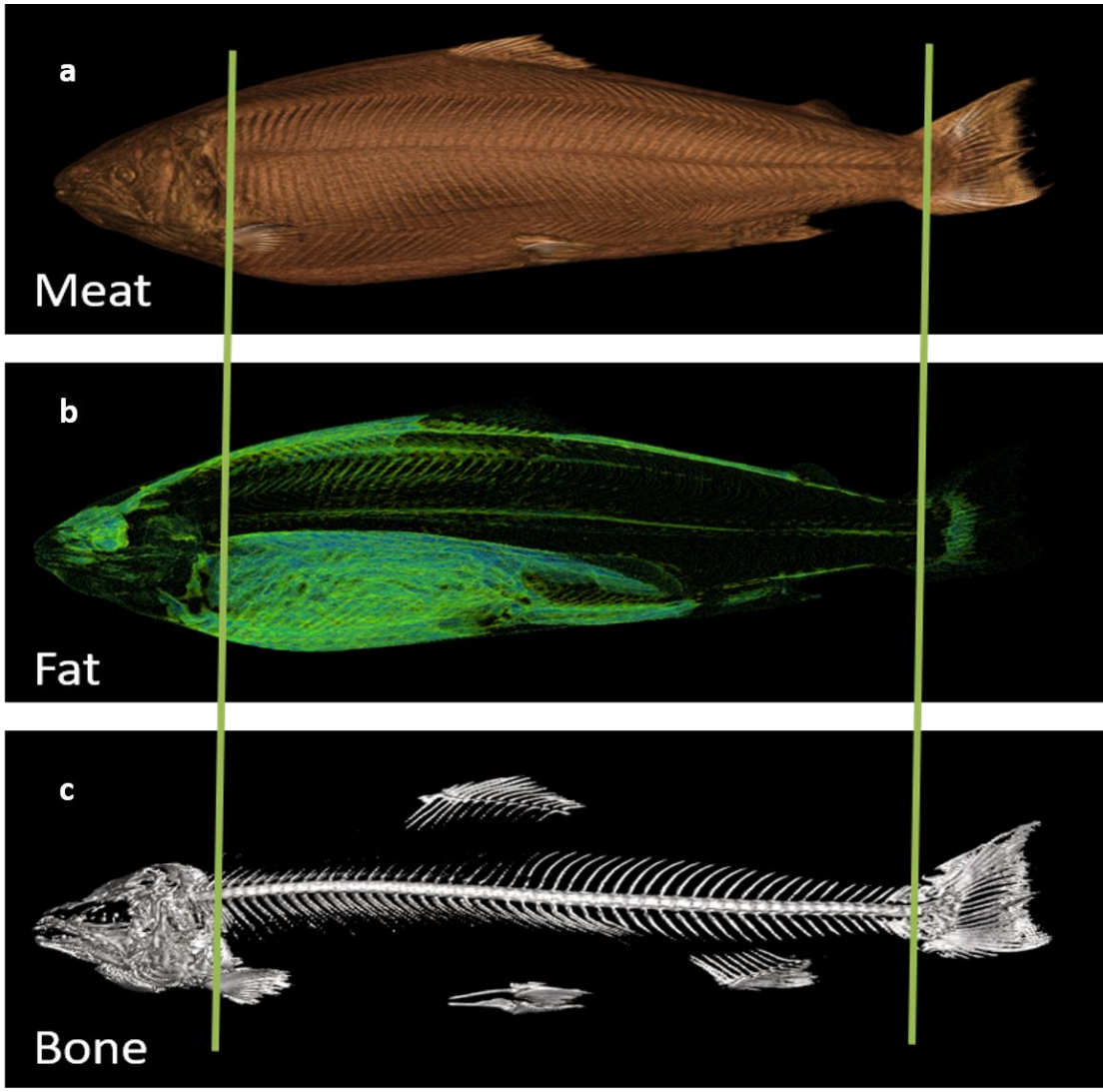


Figure 3.3 (a) The skin is removed from the CT image, (b) fatty tissue in the fillet/muscle is highlighted by a bright green colour, (c) all other tissue is stripped to remain with vertebral column and other bone structures.

The vertebral column was then divided into five distinct regions (Figure 3.4)

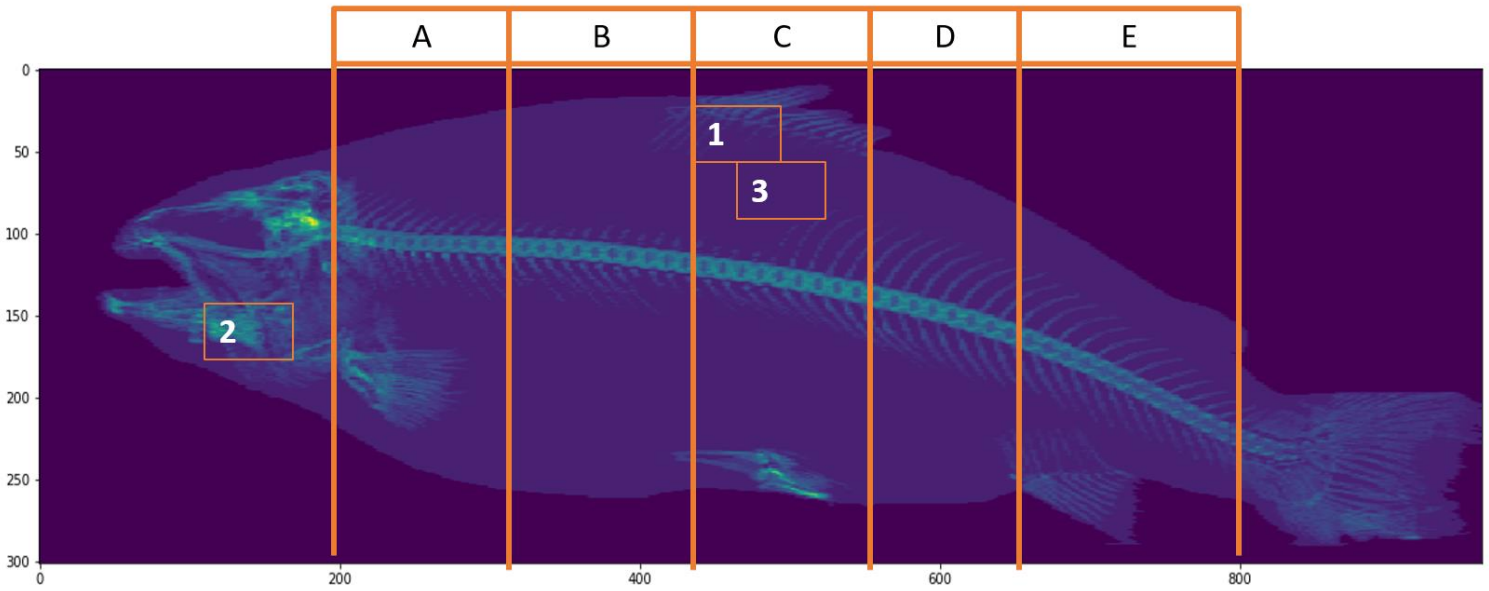


Fish 7486

Figure 3.4 division of the vertebral column into five main regions A-E. Additional regions of interest 1: Soft bone, 2: Jaw, 3: Muscle.

The definition of the regions is as follows:

Region A: Between the base of the head to the start of the dorsal fin.

Region B: From the end of region A to the start of the dorsal fin.

Region C: The region directly below the dorsal fin i.e. from the start of the dorsal fin to the end of the dorsal fin.

Region D: The region starting from the end of the dorsal fin to the start of the anal fin.

Region E: The region from the start of the anal fin to the indentation of the caudal fin.

Mineral densities of the weak bone (region 1), the strong bone (region 2) and the skeletal muscle (region 3) in addition to the selected five regions on the vertebral column were measured. These measurements were then compared amongst themselves. Bone densities greater than a set standard value may indicate malformations in the bone.

Imagej/Fiji application was used to calculate the bone mineralization. This program is an image processing program that is based on a Java script developed at the National Institutes of Health and is covered by the General Public License GPL (Rasband, 1997-2015). Ten randomly selected CT images were exported as *.png* files to *imagej* application and their colorimetric values measured as RGB colour space (Appendix A). Additional measurements were taken from the soft bone, the jaw and the muscle as indicated in Figure 3.4.

## 3.3 Physical analysis

The fish were weighed, fork length measured and scored for malformation. Thereafter the fish were gutted and the gender of the fish recorded (female salmon given the numerical identity ‘1’ and male salmon given the numerical identity ‘2’. The fish length (fork-length) was determined as the length from the tip of the snout to the indentation of the caudal fin.

Filleting was done by hand and amount of cartilage on the fillet was scored (Score 1 for presence of cartilage and score 0 for no cartilage present).

Deformities were scored from 1-3 and the approximate number of vertebrae affected counted. The CT image illustration (Figure 3.5) shows a model score chart created to identify the deformities in the sampled fish.

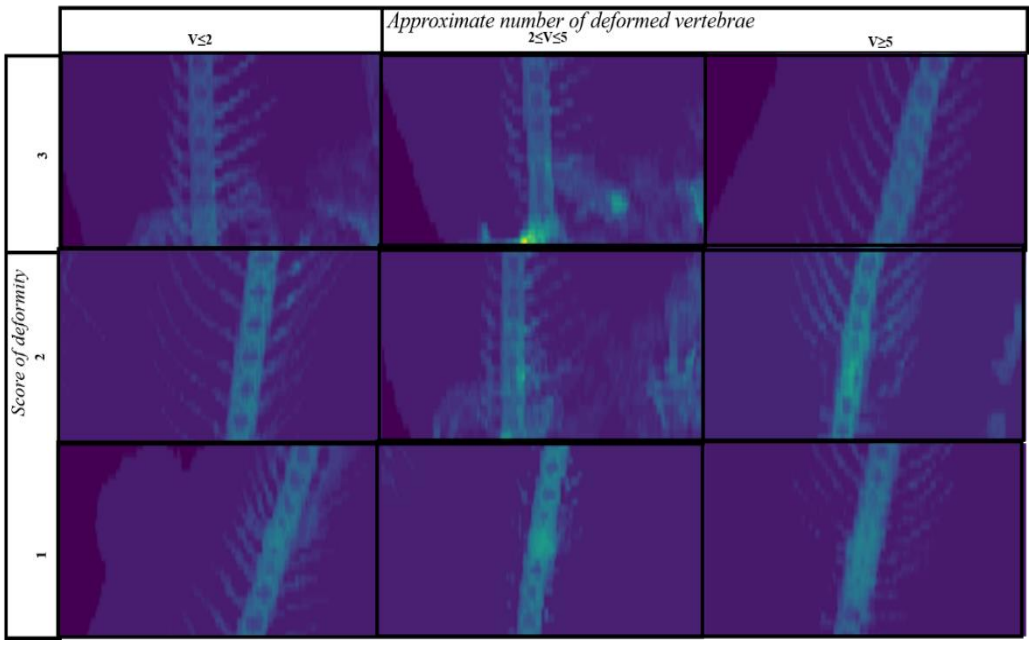


Figure 3.5 The CT images illustrate scores given on a suspected deformity from 1 to 3 and the approximate number of vertebrae affected by the deformity. Images are edited using Paint 3D, Crop Box with ration 9:16, Width of 88px and height of 156px.

## 3.4 Fillet fat content

The fillet fat content was estimated by Near InfraRed spectroscopy and given as a percentage (Folkestad, et al., 2008).

## 3.4 Statistical calculations

a) Average values of L* a* b* colorimetric values and correlations to each other (Pearson's correlation coefficient; SAS statistical software).
b) Average biometrics calculations and percentage of fish; significance level calculations (t-test).
c) Genetic and phenotypic correlation of colorimetric values and other parameters.
d) Univariate and bivariate model analysis of heritability in different parameters in study sample. The pedigreed population of 1176 fish was used to estimate the mean genetic and phenotypic values of the individuals. This was done through fitting a straight line of the genetic and phenotypic regression through points that represent on one side, the average populations genotype and phenotype and in the other side the average genotype and phenotype of the selected parents (Abplanalp, 1961).

## Heritability

A univariate linear model, was fitted to estimate genetic parameters for colorimetric variables for deformity traits (fillet deformity, vertebral deformity and number of vertebra affected). ASReml as used to estimate genetic parameters of the dependent variables. The equation for this was

$$Y = \mu + Xb + Za + e$$

Where

y=vector of phenotypic traits

μ= harvest weight as a covariate

b=vector of fixed effects of sex (male, female and unknown)

a= vector of random additive genetic effects

e= random residual effects

X and Z, = design matrices assigning observations to levels of fixed effect and additive genetic effects respectively.

A bivariate model was used to estimate genetic correlations with the variance-covariance matrices for residual and genetic structures.

The bivariate model in matrix form is shown, where subscripts 1 and 2 indicate the variables

$$\begin{pmatrix} y_1 \\ y_2 \end{pmatrix} = \mu + \begin{pmatrix} X_1 & 0 \\ 0 & X_2 \end{pmatrix} \begin{pmatrix} b_1 \\ b_2 \end{pmatrix} + \begin{pmatrix} Z_1 & 0 \\ 0 & Z_2 \end{pmatrix} \begin{pmatrix} a_1 \\ a_2 \end{pmatrix} + \begin{pmatrix} e_1 \\ e_2 \end{pmatrix}$$

All the analysis was carried out using ASReml (ASReml, 2019),

# 4 Results

The average round body weight was 4175g (range 1500g-6500g) while the average fork length was 65cm (range 50.5cm-78.5cm) with no significant difference at 5% confidence interval. The average fillet fat content was 17.9 (range12.3%-25.9%). The average condition factor was 1.59, where the males had 1.47 and the females had 1.53. Of the 1176 fish, 0.1% had no sex recorded (Table 3).

Table 3: Harvest weight, fork length and fat content in the fillet, with respect to sex. Results are given as average values and standard deviation in parenthesis.

| **Sex** | **n** | **Weight (g)** | **Length (cm)** | **Fat content (%)** |
|---|---|---|---|---|
| **Males** | 600 | 4263 (5) | 65.8 (5) | 17.9 (2) |
| **Females** | 565 | 4078(4) | 64.2 (4) | 17.6 (3) |
| **Not registered** | 11 | 4417 (3) | 65.4 (3) | 18.2 (2) |

The harvest weight and the fork length were plotted to show the distribution at slaughter time. The distribution of the harvest in grams and the distribution of the fork length in centimetres followed a normal distribution as shown in Figure 4.1.

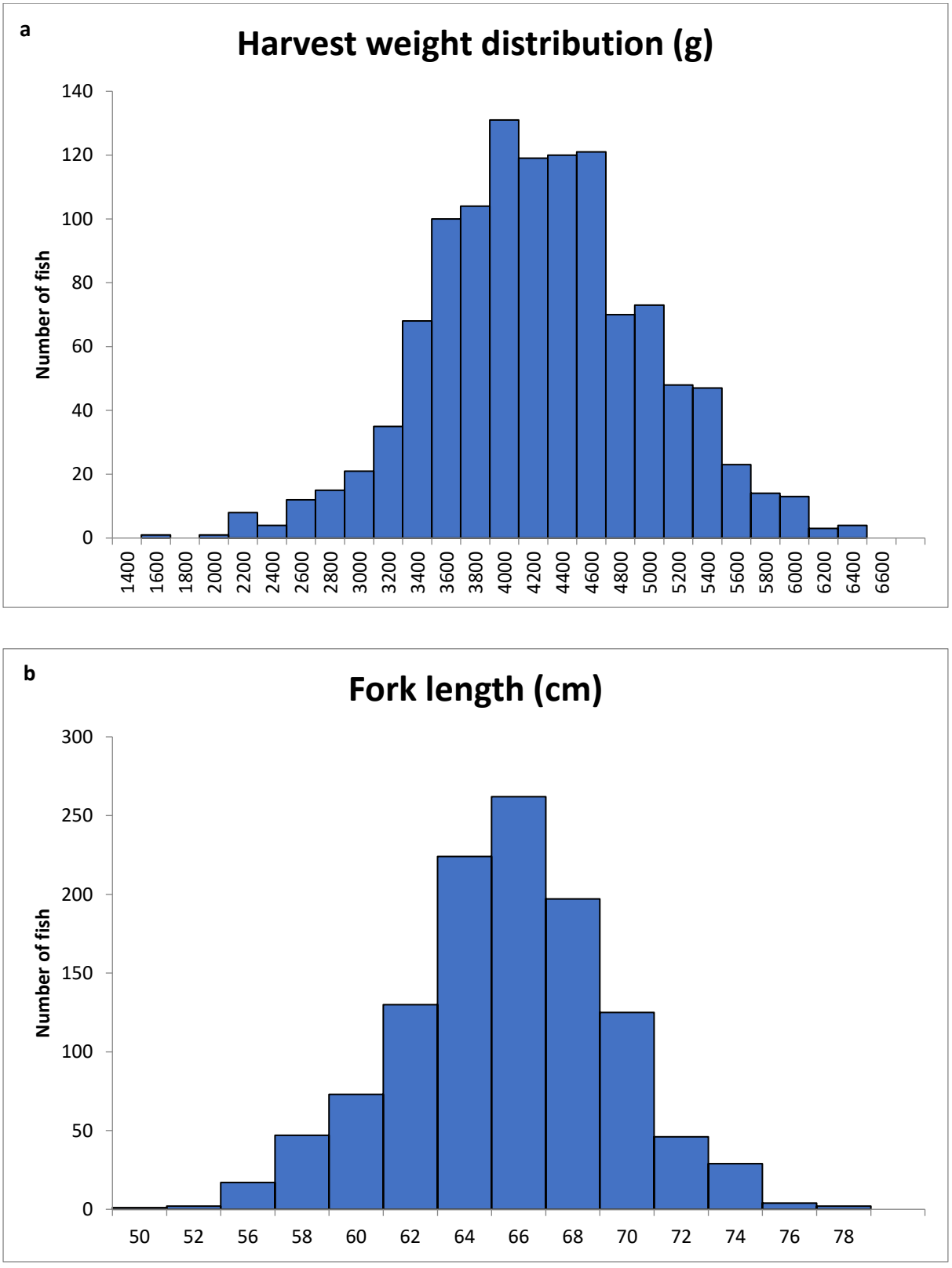


Figure 4.1 Distribution of the (a) harvest weight and (b) the fork length.

From the hypothesis test, the t value of 743.43 (to 2decimal places) was larger than the critical value of 12.71 at 5% confidence level. Hence, we reject the hypothesis that states that there is no significant difference between the harvest weights of males and females.

## 4.2 Deformity

The total number of fishes with deformities was 96 out of the 1176 sampled fish. Vertebral deformity was recorded on 8% of the fish of which 44% were male and 56% were female.

## 4.3 Colorimetric analysis

RGB parameters from imagej where transformed into XYZ by a linear regression model. They were then transformed again to L* a* b* colour space, that is how the human eye sees colour (Marty-Mahé et al., 2004). The average colorimetric values with regard to all eight regions of measurement for L*, a* and b* values were 33.0±0.07, 13.0±0.16 and -33.5±0.09 respectively.

A colorimetric correlation evaluation between the L* a* b* values was carried out in SAS and a Pearson correlation matrix was plotted (Table 4) regardless of the regions the values were measured from.

Table 4: Pearson correlation matrix of L*, a*, b* colorimetric values.

**Pearson Correlation Coefficients, N = 10584**

**Prob > |r| under H0: Rho=0**

| | **L*** | **a*** | **b*** |
|---|---|---|---|
| **L*** | 1 | -0.998<br><.0001 | 0.891<br><.0001 |
| **a*** | -0.998<br><.0001 | 1 | -0.907<br><.0001 |
| **b*** | 0.891<br><.0001 | -0.907<br><.0001 | 1 |

The Pearson's correlation analysis revealed a negative correlation between the L* and a* values (r= -0.998; p<0.0001) and the a* and the b* values (r= -0.907; p<0.0001) while the L* and b* values were positively correlated (r= 0.891; p<0.0001). The L* and a* values were so highly correlated, that focus is only given to L* value in the further reporting of the results.

Ranking of colorimetric values in relation to their correlations was done (Appendix B). It follows that, where the L*value is ranked as '1' in a specific position, the a* value is also ranked '1' as they are negatively correlated. With this information, the L* value was used as the point value for all results analysis from this point forward.

Table 5 shows the summary statistics of the colorimetric L* values. The L* values are given for regions of the vertebral column (region A-E), soft bones, jaw and the skeletal muscle (Refer to Figure 3.4 in the materials and methods chapter). Region A and B lie in the anterior part of the fish hence they became Ant_1 and Ant_2 respectively. Region C lies primarily in the middle part of the fish hence it was Mid_3. Region D and E lie in the posterior part of the fish hence

they became Post_4 and Post_5 respectively. The names of the additional three regions analysed had their names shortened and numbered.

Table 5: Descriptive statistics for the colorimetric variables L* value (n = 1176).

| | Mean | Min | Max | Std Error | Std | CV% |
|---|---|---|---|---|---|---|
| Region A: Ant_1 | 34 | 28 | 48 | 0.07 | 3 | 7 |
| Region B: Ant_2 | 36 | 29 | 52 | 0.08 | 3 | 8 |
| Region C: Mid_3 | 38 | 30 | 55 | 0.09 | 3 | 8 |
| Region D: Post_4 | 37 | 30 | 55 | 0.08 | 3 | 8 |
| Region E: Post_5 | 33 | 26 | 50 | 0.09 | 3 | 9 |
| Soft bone: Softb_6 | 23 | 20 | 28 | 0.03 | 1 | 4 |
| Jaw: Jaw_7 | 42 | 30 | 63 | 0.13 | 4 | 10 |
| Muscle: Mus_8 | 21 | 19 | 26 | 0.03 | 1 | 4 |

The L* values represent the lightness on a scale from 0 (black) -100 (white). The more positive the value, the lighter the colorimetric value. In this case, the jaw has the highest value of 42.25±4.41. This is followed by region C located in the anatomical mid region of the fish with 37.56±2.92. This is then followed by region D located in the posterior region of the fish with 37.09±2.88. This is followed by region B in the anterior region of the fish with 35.76±2.68. This is followed by region A also in the anterior part of the fish with 34.39±2.50. Then comes region E in the posterior end of the fish with 33.39±2.97. This is then followed by the soft bone with 22.52±0.99. Lastly, the muscle has the lowest L* value mean of 21.27±0.86 (Appendix C).

Figure 4.3 shows the distribution of the L* values along the vertebral column and the soft bone, jaw and muscle regions of Atlantic salmon. The mean L* values in these regions follows a normal distribution.

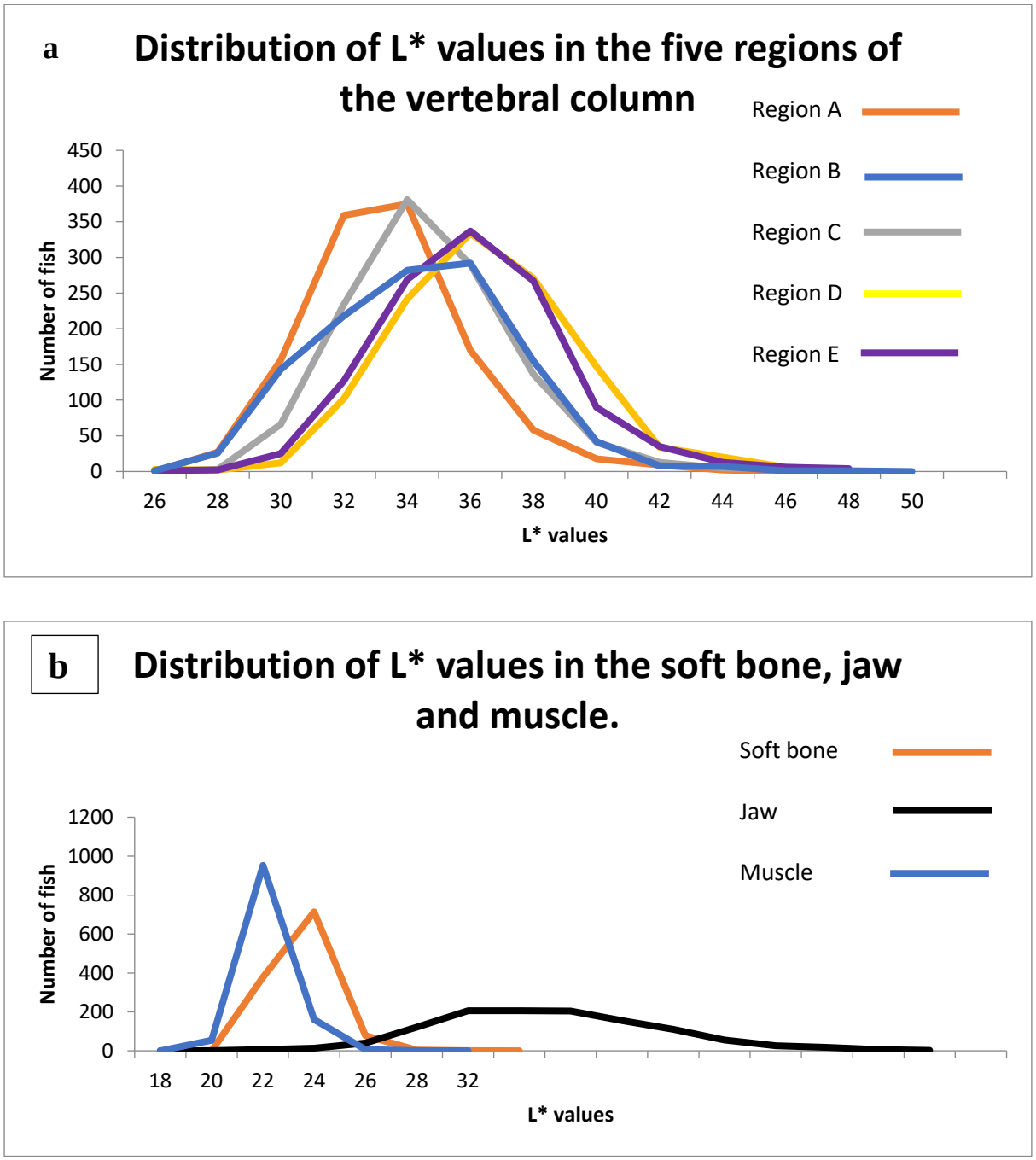


Figure 4.3 (a) Distribution of the L* values for the regions A – E (b) Distribution of the L* values for the soft bone, jaw and muscle regions.

With focus on the L* value as a dependent variable, a t-test was done to find evidence of significant differences in the colorimetric values of the eight regions of whole fish. The coefficient of determination was R=0.863. This showed that 86.3% of the variation in the L* values can be attributed to the position in which it was measured from (Appendix D).

The significance of the L* colorimetric values with regards to the position of measurements was calculated using SAS© and a comparison figure was plotted. Figure 4.4 shows the average L* values for the different positions. The L* values differed significantly among all the positions (P<0.05).

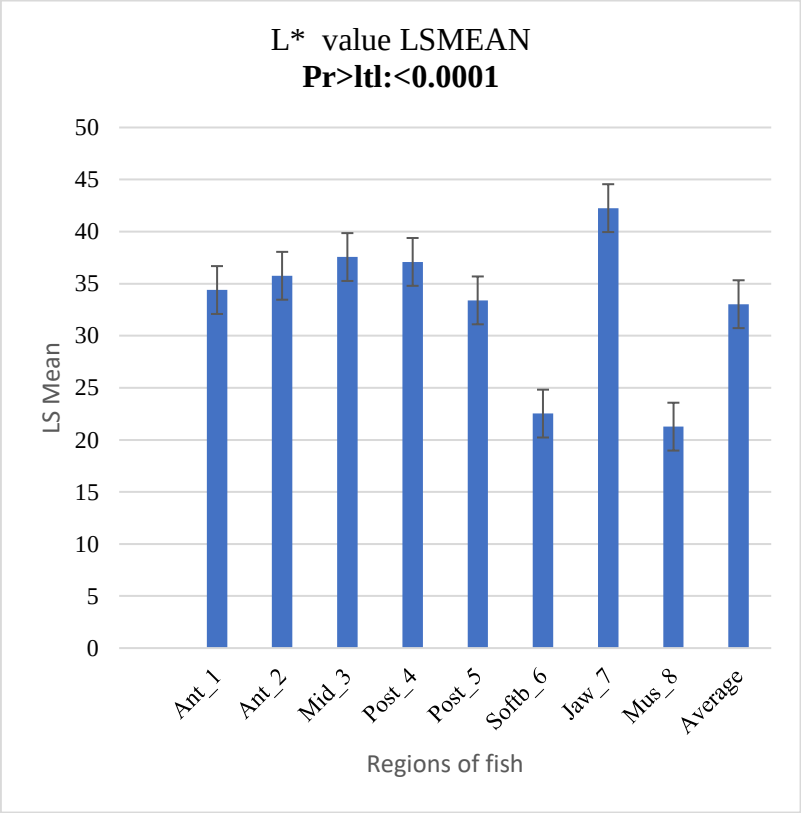


Figure 4.4 Least Squares mean of regions of fish for the L* colorimetric value with their standard errors (Appendix C).

Estimates or predicting how the dependent variable (L* colorimetric values) behaves in relation to the position it has been measured from can be seen in Figure 4.4. On the L* value, the soft bone and the muscle show a larger difference in the colorimetric values as compared to the other regions. From the image analysis, these two regions appear darker compared to the other regions.

The significant differences in the colorimetric values between regions led to calculation of the correlations of the L* values between the regions. Table 6 shows the phenotypic correlations above the diagonal and genetic correlations below the diagonal for the L* colorimetric values

with regards to region of measurement for region A-E as well as the soft bone, jaw and the muscle.

Table 6 The genetic correlations for L* values below the diagonal, and the phenotypic correlations above the diagonal. The values in parenthesis indicate the P value, where * indicates P<0.0001.

| | **Region A** | **Region B** | **Region C** | **Region D** | **Region E** | **Soft Bone** | **Jaw** | **Muscle** |
|---|---|---|---|---|---|---|---|---|
| **Region A** | **1 (NE)** | 0.83* | 0.83* | 0.79* | 0.72* | 0.74* | 0.41* | 0.78* |
| **Region B** | 0.99 (0.02) | **1 (NE)** | 0.85* | 0.80* | 0.71* | 0.75* | 0.42* | 0.80* |
| **Region C** | 0.97 (0.02) | 0.98 (0.02) | **1 (NE)** | 0.86* | 0.73* | 0.77* | 0.43* | 0.82* |
| **Region D** | 0.99 (0.01) | 0.98 (0.02) | 0.99 (0.01) | **1 (NE)** | 0.79* | 0.75* | 0.43* | 0.80* |
| **Region E** | 0.94 (0.05) | 0.98 (0.05) | 0.96 (0.05) | 0.98 (0.04) | **1 (NE)** | 0.62* | 0.51* | 0.69* |
| **Soft Bone** | 1 (0.03) | 0.92 (0.04) | 0.90 (0.04) | 0.94 (0.03) | 0.96 (0.06) | **1 (NE)** | 0.38* | 0.92* |
| **Jaw** | 0.54 (0.18) | 0.62 (0.16) | 0.56 (0.17) | 0.52 (0.17) | 0.53 (0.21) | 0.61 (0.17) | **1 (NE)** | 0.37* |
| **Muscle** | 1 (NE) | 0.95 (0.03) | 0.94 (0.03) | 0.96 (0.03) | 0.95 (0.06) | 0.98 (0.01) | 0.54 (0.18) | **1 (NE)** |

The phenotypic correlation of the L* values between the regions shows lower correlations between the jaw and the other regions. These range from r= 0.38 with the soft bone to r=0.51 with region E. The highest phenotypic correlation is between region C and region D (r=0.86). The genetic correlations of the jaw compared to the other regions is also lower ranging from r=0.52 with region D to r=0.62 with region B. Region C and region D are amongst the highest genetic correlations, r= 0.99.

Table 7 shows the summary statistics of the colorimetric b* values. The b* values are given for regions of the vertebral column (region A-E), soft bones, jaw and the skeletal muscle (Refer to Figure 3.4 in the materials and methods chapter).

Table 7: Descriptive statistics for the colorimetric variables b* values (Yellow/Blue Values) (n = 1176).

| | Mean | Min | Max | Std Error | Std | CV |
|---|---|---|---|---|---|---|
| Region A: Anterior 1 | -35 | -40 | -15 | 0.08 | 3 | -8 |
| Region B: Anterior 2 | -33 | -39 | 22 | 0.18 | 6 | 82 |
| Region C: Mid | -31 | -39 | -2 | 0.11 | 4 | -12 |
| Region D: Posterior 1 | -31 | -39 | -4 | 0.10 | 4 | -11 |
| Region E: Posterior 2 | -35 | -40 | -13 | 0.09 | 3 | -8 |
| Soft bone | -40 | -41 | -38 | 0.01 | 0 | -1 |
| Jaw | -24 | -39 | 16 | 0.2 | 7 | -28 |
| Muscle | -39 | -41 | -37 | 0.02 | 1 | -1 |

The b* values represent the colours yellow or blue on the y-axis, i.e. the more positive the b* value is, the more yellowish it is the image, while the more negative b* values, the more bluish is the image. In this case, all the b* values were negative indicating that the image will appear bluer to the human eye. The soft bone had the lowest value of -39.67±0.42. This is followed by the muscle with -39.00±0.53. This is then followed by region E located in the posterior

region of the fish with -35.42±2.97. This is followed by region A in the anterior region of the fish with -34.78±2.74. This is followed by region B also in the anterior part of the fish with -33.08±6.15. Then comes region D in the posterior end of the fish with -31.27±3.56. This is then followed by the region C with -30.82±3.71. Lastly, the jaw has the highest b* value mean of -23.86±6.78 (Appendix C).

Figure 4.5 and 4.6 show the distribution of the b* values along the vertebral column and the soft bone, jaw and muscle regions of Atlantic salmon. The mean L* values in these regions follows a normal distribution.

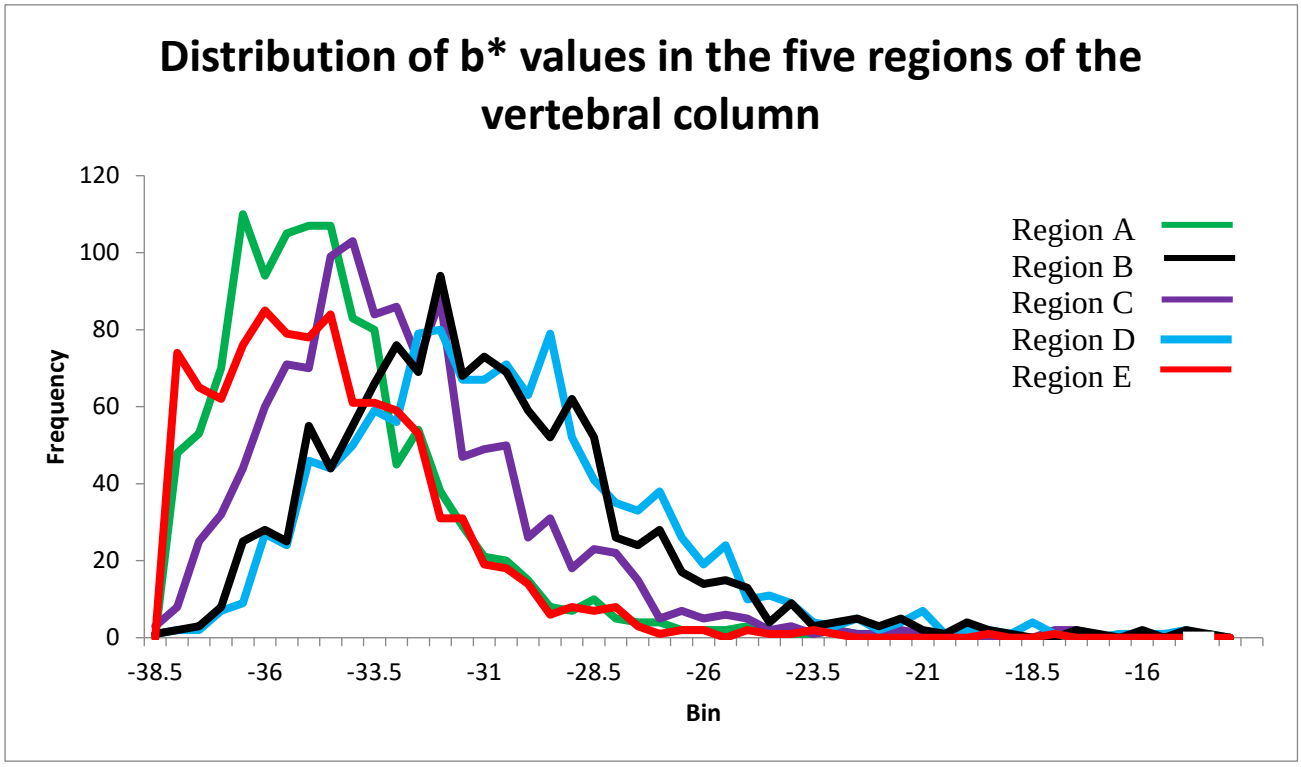


Figure 4.5 Distribution of the b* values for the regions A – E.

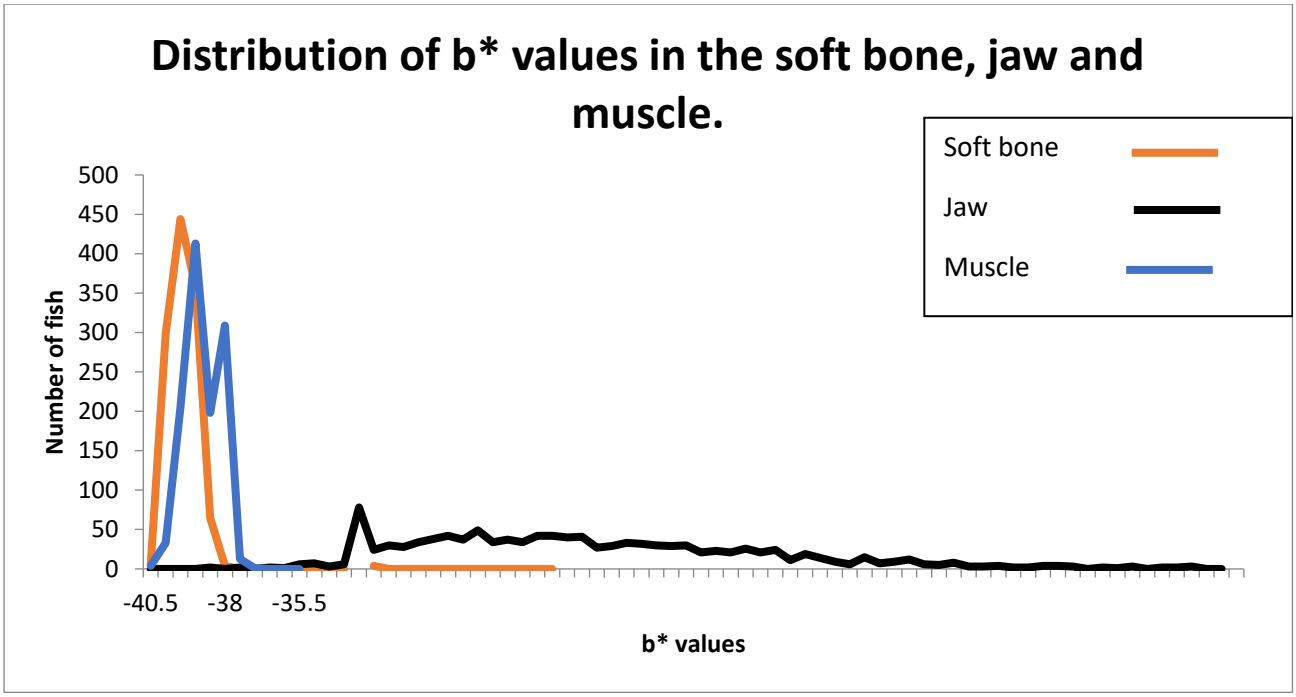


Figure 4.6 Distribution of the b* values for the soft bone, jaw and muscle regions.

With focus on the b* value as a dependent variable, a t-test was done to find evidence of significant differences in the colorimetric values of the eight regions analysed. The coefficient of determination was R=0.631. This showed that 63.1% of the variation in b* colorimetric values was be attributed to the position in which it was measured from (Appendix D).

The significance of the b* colorimetric values with regards to the position of measurements was calculated using SAS© and a comparison figure was plotted. Figure 4.7 shows the average values of the b* values for the different positions.

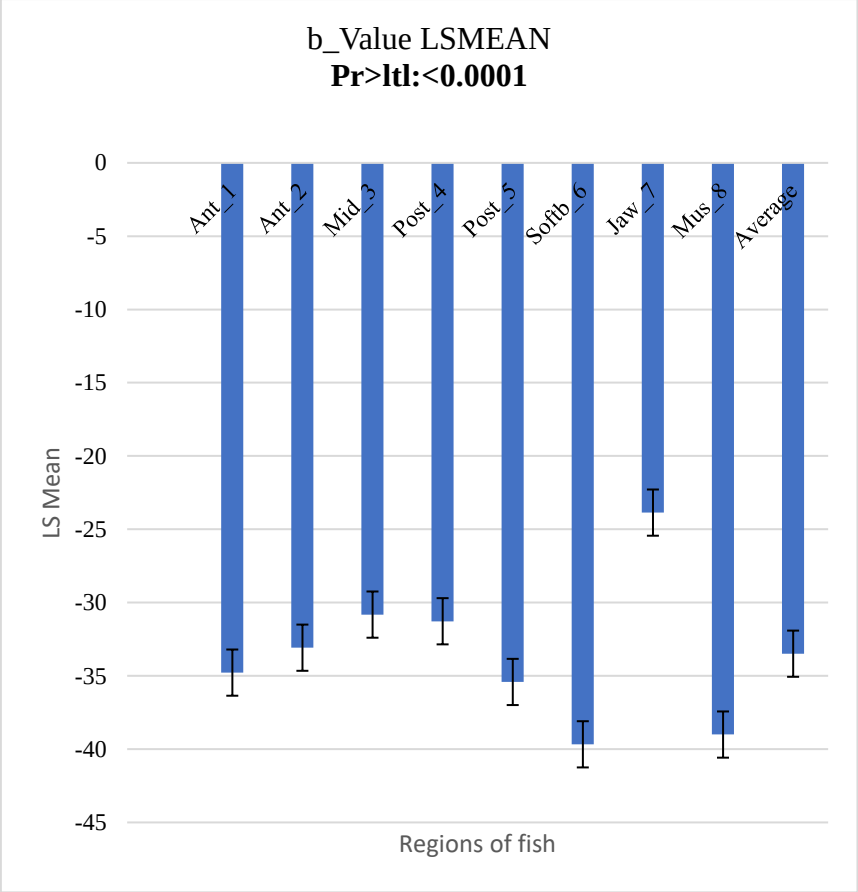


Figure 4.7 Least Squares mean of regions of fish for the b* colorimetric value.

The b* value of the soft bone and the muscle show the lowest values as compared to the other regions. From the image analysis, these two regions appear bluer compared to the other regions. The significant differences in the colorimetric values between regions led to calculation of the correlations of the b* values between the regions. Table 8 shows the phenotypic correlations above the diagonal and genetic correlations below the diagonal for the b* colorimetric values with regards to region of measurement for region A-E as well as the soft bone, jaw and the muscle.

Table 8 The genetic correlations for b* values below the diagonal, and the phenotypic correlations above the diagonal. The values in parenthesis indicate the P value, where * indicates P<0.0001.

| ***b*value*** | **Region A** | **Region B** | **Region C** | **Region D** | **Region E** | **Soft Bone** | **Operculum** | **Muscle** |
|---|---|---|---|---|---|---|---|---|
| **Region A** | **1 (NE)** | 0.83* | 0.86* | 0.84* | 0.76* | -0.70* | 0.44* | -0.75* |
| **Region B** | 0.99 (0.02) | **1 (NE)** | 0.89* | 0.86* | 0.77* | -0.71* | 0.46* | -0.77* |
| **Region C** | 0.97 (0.02) | 0.98 (0.01) | **1 (NE)** | 0.90* | 0.78* | -0.73* | 0.46* | -0.79* |
| **Region D** | 0.97 (0.02) | 0.98 (0.01) | 0.99 (0.01) | **1 (NE)** | 0.83* | -0.71* | 0.47* | -0.78* |
| **Region E** | 0.96 (0.04) | 0.98 (0.04) | 0.96 (0.04) | 1 (0.03) | **1 (NE)** | -0.57* | 0.53* | -0.66* |
| **Soft Bone** | -1 (NE) | -0.96 (0.04) | -0.92 (0.04) | -0.95 (0.36) | -1 (NE) | **1 (NE)** | -0.35* | 0.91* |
| **Operculum** | 0.59 (0.17) | 0.63 (0.15) | 0.6 (0.15) | 0.58 (0.15) | 0.63 (0.17) | -0.68 (0.15) | **1 (NE)** | -0.37* |
| **Muscle** | -0.99 (0.03) | -0.98 (0.02) | -0.94 (0.03) | -0.97 (0.03) | -1 (NE) | 0.96 (0.03) | -0.63 (0.16) | **1 (NE)** |

The phenotypic correlation for the b* values between the regions shows lower correlations between the jaw and the other regions. These range from r= -0.35 with the soft bone to r= 0.53 with region E. The highest positive phenotypic correlation is between the soft bone and the muscle (r=0.91) and the highest negative phenotypic correlation is between the muscle and region C (r= -0.79). The genetic correlations of the jaw compared to the other regions is ranging from r=-0.68 with the soft bone to r=0.63 with region B and region E. The highest genetic correlations, r= 1(0.03) is between Region D and region E.

## 4.4 Heritability

The phenotypic and genetic parameters of the L* values are shown in Table 9

Table 9: Estimates of genetic variance ($\sigma_A^2$), phenotypic variance ($\sigma_P^2$) and heritability ($h^2_x$) with their standard errors in parenthesis (s.e.) for L*values for the different regions of the fish, N=1176.

| **Traits** | **$\sigma_A^2$(s.e.)** | **$\sigma_P^2$(s.e.)** | **$h^2_1$ (s.e.)** | **$h^2_2$ (s.e.)** |
|---|---|---|---|---|
| **Region A** | 1.41 (0.37) | 6.29(0.28) | 0.23 (0.05) | 0.23 (0.06) |
| **Region B** | 2.71 (0.51) | 7.29 (0.34) | 0.31 (0.06) | 0.33 (0.06) |
| **Region C** | 2.76 (0.61) | 8.61 (0.40) | 0.32 (0.06) | 0.34 (0.06) |
| **Region D** | 2.62 (0.59) | 8.37 (0.39) | 0.31 (0.06) | 0.33 (0.06) |
| **Region E** | 1.08 (0.40) | 8.82 (0.38) | 0.12 (0.04) | 0.12 (0.05) |
| **Soft bone** | 0.26 (0.63) | 0.98 (0.04) | 0.27 (0.06) | 0.28 (0.06) |
| **Jaw** | 1.81 (0.80) | 19.48 (0.82) | 0.09 (0.04) | 0.11 (0.04) |
| **Muscle** | 0.20 (0.48) | 0.74 (0.03) | 0.27 (0.06) | 0.33 (0.06) |
| **L* average** | 1.16 (0.28) | 4.46 (0.20) | 0.26 (0.06) | 0.29 (0.06) |

$h^2_1$= Heritability

$h^2_2$= Heritability with harvest weight as a covariate

The phenotypic and genetic parameters of the b* values estimated from univariate analysis are shown in Table 10.

Table 10: Estimates of genetic variance ($\sigma_A^2$), phenotypic variance ($\sigma_P^2$) and heritability ($h^2_x$) with their standard errors in parenthesis (s.e.) for b*values for the different regions of the fish, N=1176.

| **Traits (b*)** | **$\sigma_A^2$(s.e.)** | **$\sigma_P^2$(s.e.)** | **$h^2_1$ (s.e.)** | **$h^2_2$ (s.e.)** |
|---|---|---|---|---|
| **Region A** | 1.62 (0.43) | 7.5 (0.33) | 0.21 (0.05) | 0.23 (0.05) |
| **Region B** | 3.28 (0.72) | 10.16 (0.48) | 0.32 (0.06) | 0.35 (0.07) |
| **Region C** | 4.5 (0.98) | 13.83 (0.65) | 0.33 (0.06) | 0.35 (0.06) |
| **Region D** | 4.03 (0.89) | 12.81 (0.60) | 0.31 (0.06) | 0.33 (0.06) |
| **Region E** | 1.24 (0.43) | 8.84 (0.38) | 0.14 (0.05) | 0.15 (0.05) |
| **Soft bone** | 0.05 (0.12) | 0.18 (0.01) | 0.28 (0.06) | 0.29 (0.06) |
| **Jaw** | 4.91 (1.96) | 46.11 (1.95) | 0.11 (0.04) | 0.12 (0.04) |
| **Muscle** | 0.08 (0.18) | 0.28 (0.01) | 0.27 (0.06) | 0.31 (0.06) |
| **b* average** | 1.3 (0.33) | 5.48 (0.25) | 0.24 (0.06) | 0.26 (0.06) |

$h^2_1$= Heritability

$h^2_2$= Heritability with harvest weight as a covariate

In the bivariate analysis, genetic parameters were estimated for all traits. The region D compared to the other L* values/b* values was considered as this area corresponds to the Norwegian Quality Cut (NQC) and is of specific interest. The genetic correlations for the L*values and b* values were plotted in the lower diagonal of the matrices in Appendix E and Appendix F respectively. The bivariate heritability of the L* values and b*values were plotted on the diagonal of the respective matrices.

The phenotypic and genetic parameters of the fillet deformity, vertebral deformity and number of vertebrae affected estimated from univariate analysis are shown in Table 11.

Table 11 Estimates of genetic variance ($\sigma_A^2$), phenotypic variance ($\sigma_P^2$) and heritability ($h^2$) with their standard errors in parenthesis (s.e.) for fillet deformity, vertebral deformity and number of vertebrae affected, N=1176.

| **Traits** | **$\sigma_A^2$** **(s.e.)** | **$\sigma_P^2$** **(s.e.)** | **$h^2$** **(s.e.)** | **$h^2_w$** **(s.e.)** |
|---|---|---|---|---|
| **Fillet Deformity** | 0.01 (0.33) | 0.08 (0.03) | 0.08 (0.04) | 0.07 (0.04) |
| **Vertebral Deformity** | 0.01 (0.69) | 0.19 (0.01) | 0.05 (0.04) | 0.04 (0.03) |
| **Number of Vertebra affected** | 0.93 (0.85) | 25.50 (1.06) | 0.04 (0.03) | 0.03 (0.03) |

The heritability for the fillet deformity, vertebral deformity and the number of vertebrae affected was low and so their genetic correlations to the average L* and b* colorimetric values were calculated. Table 12 shows the genetic correlation of these trait variable and the colorimetric values with the standard errors in parenthesis.

Table 12: Genetic correlations of trait variables to L* values and b* values averages (Standard Error).

| | **L* average** | **b* average** |
|---|---|---|
| **b* average** | 1 (NE) | . |
| **Fillet Deformity** | -0.15 (0.25) | -0.82 (0.25) |
| **Vert Def** | 0.23 (0.3) | 0.29 (0.3) |
| **No of Vertebra** | 0.36 (0.33) | 0.45 (0.33) |

NE*: Standard Error Estimates from bivariate model are Not Estimable*

# 5 Discussion

It is known that the denser the tissue or bone is, the lighter it will appear on a CT image (Kak & Slaney, 1988). Upon measuring the L* values on the images, the jaw which is denser than the muscle may appears lighter and has a more positive L* value. When compared to the jaw, muscle shows a lower L* colorimetric value unit, indicating a darker appearance. Consequently, the denser a tissue is, the higher the L* value, the lower the a* value and this signifies a higher mineral content in a region of interest. The results from this study therefore indicate decreasing mineralisation of the vertebra from head to tail.

The mineralisation (L* values) correlated significantly between different regions along the vertebral column, indicating that a defined area could be used for predicting mineral deposition; for example the Norwegian Quality Cut that is a standard cutlet between the posterior part of the dorsal fin and the gut, commonly used for fillet quality analysed (NS9401, 1994). Previous studies have documented that bone mineralisation can be predicted using CT scanning and predict the onset of osteoporosis thereby reducing the risk of lordosis or fractures in the bone (Kyung Joon, et al., 2019).

However, the present results are the first to show such comprehensive study of different regions along the vertebral spine of Atlantic salmon. Moreover, this study shows for the first time a significant correlation between predicted mineral deposition in the skeleton and the muscle. Hence it can be suggested that mineral deposition in bones and skeletal muscle can be predicted by either using whole fish (possibly even live fish) or by performing the measurements on a standard cutlet, such as the NQC (Kyung Joon, et al., 2019).

A deformed fish has one or more vertebrae affected (Sambraus, et al., 2014). With this definition, 8.2% fish were classified as deformed. It should be noted that in this study, there is no decisive evidence to conclude that some of the observed vertebral deformity are breaks in the vertebral column or cartilage. Less than 5 fish in total had hat appeared to be a break in the vertebral column. Speculating that it is a break in the vertebral column can be attributed to how the fish were killed or handled before analysis. Because the fish were going to be sold for public consumption, electric stunning was used as a method of slaughter. Thus, in this study, the method used to euthanise the fish had no implication on the analysis.

From the graphs plotted, the trend in the different parameters from the L* values in the different five main regions and including the harvest weight and fork length, the data showed that it statistically followed a normal distribution. The behaviour of the extra three regions, soft bone, jaw and muscle was also studied. The L* value for the soft bone was lower as compared to the other two samples.

The condition factor, (1.59) showed these fish were at the high end of what is considered good quality and in good health, which is supported by a CF calculation chart of salmonids (Barnham & Baxter, 1998). On the slaughter days, there were rotations of people in the workstation made it difficult to pair the fillet to the filleter and hence this effect was discarded when considering fillet scoring.

The average heritability for the L* values was 0.26 with a standard error of 0.06, which is considered significant and moderate. Of the total 1176 fish, the most heritable region was determined to be region C by the L* value estimation of heritability of 0.32 with a standard error of 0.06. This was the same case when heritability was estimated with the weight as a covariate. The inclusion of weight was significant ($p<0.0001$). As the phenotypic correlations indicated that L* and a* values were almost identical, I prioritized estimating genetic parameters for L* and b* only.

The average heritability for the b* values was 0.24 with a standard error of 0.06. Of the total 1176 fish, the most heritable region was also the region C by the b* value estimation of 0.33 with a standard error of 0.06. The heritability of this same region with weight as a covariate was 0.35 with a standard error of 0.06. The inclusion of weight was significant ($p<0.0001$).

Bone mineral densities of the different regions of the fish from both the L* and b* values as estimated in ASReml are moderately heritable. This suggests a contribution of additive genetic effect, and that if relevant, selective breeding for these traits is possible. Genetic correlation of the average L* values and average b* values was estimated, showing the two are positively correlated with a non-estimable standard error.

Fillet deformity, vertebral deformity and the number of vertebrae affected have heritability of 0.08, 0.05 and 0.04 respectively. These low heritability's may indicate that although malformations are genetically predisposed, they can only be commonly expressed under unnatural conditions for the fish for example high water temperatures or very high oxygenation in the tanks. This is the same with a previous study showing the heritability of skeletal

deformity being close to zero in different families and only rising in the different clusters when routine management practises were altered (Kause, et al., 2007). Another reason for the low heritability in these traits could be due to a low genetic variance. Although the traits are predetermined by genetics, they are a common occurrence and their variation is thus low (Oldenbroek & Waaij, 2014). In previous studies, the observed heritability's in 4 different year-classes differs. It ranged from 0.00±0.00 to 0.20±0.08 showing variation in the individuals from the same families (Gjerde, et al., 2005).

All the genetic correlations calculated between the L* values are positive. The regions with a significantly higher relationship genetically with region D (Norwegian Quality Cut) are from region A to region E as well as the soft bone and muscle. The region with a lower but still significant genetic correlation with the region D is the jaw. The genetic correlations calculated for the b* values are positive for the region A to region E. their relationship is significantly higher to the region D (NQC). The soft bone and muscle have a significantly negative genetic correlation of b* values with the NQC region. The region with a significantly lower genetic correlation with respect to the NQC region is the jaw. Based on this study, region D or the NQC which is already a standard in the industry can be used to measure the mineralisation of the bones. Alternatively, region C located just below the dorsal fin can be used as a region of interest as the heritability of thesis region is higher than all the other regions.

# 6 Conclusion

A novel method for predicting Atlantic salmon bone mineralization was developed based on highly sensitive and advanced equipment-Computed Tomography and image analyses (Cie-lab colorimetric parameters). Mineralization differed significantly between anatomical regions with the jaw having the highest mineralized bone. The soft bones attaching the dorsal fin to the fillet and the skeletal muscle had the lowest mineral concentration. The vertebral column showed decreasing mineral concentration from head to tail

The bone mineral density, as presented by the L* and b* values, is moderately heritable ($h^2$ =0.21-0.33; for the jaw $h^2$ =0.09-0.11). The phenotypic variance observed in Atlantic salmon in this study was due to genetics as well as the genetics by environmental factors.

The region of the vertebral column showing the highest heritability was the area below the dorsal fin (region C: $h^2$=0.32 for the L*value and $h^2$=0.33 for the b*value). Heritability of predicted mineral deposition of the skeletal muscle in the same region was $h^2$=0.27 (L* and b* value). Hence, mineral deposition can be predicted in both bones and skeletal muscle by performing analysis in the region below the dorsal fin and implemented in breeding programs or alternatively in region D, the Norwegian Quality Cut.

The fillet deformity, vertebral deformity and number of vertebrae affected showed low heritability's. Their effect in a breeding plan for Atlantic salmon in this pedigree is negligible.

This study was based on bone mineral density determination through colorimetric analysis of the skeleton and muscle. There is need for future studies using the chemical analysis and the mechanical analysis to confirm the correlation between the Cie-lab colorimetric values and the Hounsfield Units.

This method of bone mineral density determination can be further developed to measure reductions in specific minerals that may result in shortening of the vertebral column, weakening of the bone, enlargement of the head or assimilation of cartilage in the eye and optic capsules malformations of Atlantic salmon. Thus, it is possible to predict and identify malformations in the vertebral column of Atlantic salmon using CT scan.

# 7 References

Abplanalp, H., 1961. Linear heritability estimates. *Genetical Research,* 2(3), pp. 439-448 doi:10.1017/S0016672300000926.

ASReml, 2019. *version 4.0,* [1 January 2013] to [1 January 2014]; Expiry 31 March 2020: registered to Akvaforsk Genetics Center AS, Serial Number 402080577.

Baeverfjord, G., 1999. *Deformities induced by temperature stress in farmed Atlantic salmon and Rainbow trout,* s.l.: Report to the Norwegian Research Council of Norway, pp. 19..

Baeverfjord, G., Asgard, T. & Shearer, K., 1998. *Development and detection of phosphorus deficiency in Atlantic salmon, Salmosalar L., parr and post-smolts.* s.l.:Aquaculture Nutrition, 4: 1–11.doi:10.1046/j.1365-2095.1998.00095.x.

Balon, E. K., 1995b. The common carp, Cyprinus carpio: its wild origin, domestication in aquaculture, and selection as colored nishikigoi. Volume 3, pp. 1-55.

Barnham, C. P. & Baxter, A., 1998. Condition Factor, K, for Salmonid Fish. *Fisheries Notes,* FN0005(ISSN 1440-2254).

Berillis, P., 2015. Factors that can lead to the development of skeletal deformities in fishes: A review. *Journal of FisheriesSchience.com.*

Bucke, D. & Andrews, C., 1985. *Vertebral abnormalities in chub, Leuciscus(Squalius) cephalus L.* s.l.:Bulletin of the European Association of Fish Pathologists, 5(1), 3-5..

Buzug, T. M., 2008. *Computed Tomography: From Photon Statistics to Modern Cone-Beam CT.* First ed. Berlin: Springer-Verlag Berlin Heidelberg.

Canadian Environmental Sustainability Indicators, 2011. *Freshwater Quality Indicator: Data Sources and Methods.* Catalogue Number En4-144/1-2011E-pdf, ISBN 978-1-100-17976-6. ed. s.l.:Environment Canada.

Celenk, C. & Celenk, P., 2008. Bone Density Measurement Using Computed Tomography. In: *Computed Tomography – Clinical Applications.* Turkey: s.n., pp. 123-136.

Chatain, B., 1994. *Abnormal swimbladder development and lordosis in sea bass (Dicentrarchuslabrax) and sea bream (Sparusauratus). Aquaculture, 119(4), 371-379.doi:10.1016/0044-8486(94)90301-8.* s.l.:s.n.

CIE, 1976. *L*a*b* colour space.,* s.l.: s.n.

Cobcroft, J. & Battaglene, S., 2009. *Jaw malformation in striped trumpeter Latrislineata larvae linked to walling behaviour and tank colour.* s.l.:Aquaculture, 289(3): 274-282.doi:10.1016/j.aquaculture.2008.12.018..

Dalsgaard, I. & Madsen, L., 1999. Vertebral column deformities in farmed rainbow trout ( Oncorhynchus mykiss ). *Aquaculture*, 171(1-2), pp. 41-48.

Davies, P., J.P, G. J., Sinley, J. & Smith, N., 1976. *Acute and chronic toxicity of lead to rainbow trout Salmogairdneri in hard and soft water.* s.l.:Water Research, 10(3): 199-206.doi:10.1016/0043-1354(76)90128-7.

Dedi, J. et al., 1997. *Hypervitaminosis A during vertebral morphogenesis in larval Japanese flounder.* s.l.:Fisheries Science, 63: 466–473.

Dempster, E. R. & Lerner, I. M., 1950. Heritability of Threshold Characters. *Genetics,* 35(2), pp. 212-236.

Devlin, E., 2006. *Acute toxicity, uptake and histopathology of aqueous methyl mercury to fathead minnow embryos.* s.l.:Ecotoxicology, 15: 97–110.doi:10.1007/s10646-005-0051-3.

Dingerkus, G. & Uhler, L. D., 1977. Enzyme clearing of alcian blue stained whole small vertebrates for demonstration of cartilage.. *Stain Technol, ,* 52(4 doi:10.3109/10520297709116780), pp. 229-232.

Divanach, P. et al., 1996. Abnormalities in finfish mariculture: an overview of the problem, causes and solutions. In: B. Chatain, M. Saroglia, J. Sweetman & P. Lavens, eds. *Seabass ans Seabream Culture: Problems and Prospects FAS International Workshop.* Verona, Italy: s.n., pp. 45-66.

Eggset, G., Mortensen, A. & Løken, S., 1999. Vaccination of Atlantic salmon (Salmo salar L.) before and during smoltification; effects on smoltification and immunological protection. *Aquaculture,* 170(2), pp. 101-112.

Eknath, A. et al., 1991. *Approaches to national fish breeding programs – Pointers from tilapia pilot,* Research Gate: ICLARM contribution No. 723.

EU JRC, 2018. *How much fish do we consume? First global seafood consumption footprint published,* s.l.: EU Science Hub.

Exploring our fluid Earth, Accessed 2019. *https://manoa.hawaii.edu/exploringourfluidearth/biological/fish/structure-and-function-fish,* s.l.: Teaching Science as inquiry.

FAO, 2012. *The state of world fisheries and aquaculture,* Rome: FOOD AND AGRICULTURE ORGANIZATION OF THE UNITED NATIONS.

FAO, 2013. *FISH TO 2030, Prospects for Fisheries and Aquaculture,* WORLD BANK REPORT NUMBER 83177-GLB: AGRICULTURE AND ENVIRONMENTAL SERVICES DISCUSSION PAPER 03.

FAO, 2016. The state of world fisheries and aquaculture, Contributing to food security and nutrition for all. *Food and Agriculture Organisation of the United Nations,* p. 200pp.

Ferguson, M. M. & Danzmann, R. G., 1995. Role of genetic markers in fisheries and aquaculture: Useful tools or stamp collecting?. *Canadian Journal of Fisheries and Aquatic Sciences,* 55(7), pp. 1553-1563.

Fernández, I. et al., 2008. *Larval performance and skeletal deformities in farmed gilthead sea bream (Sparusaurata) fed with graded levels of Vitamin A enriched rotifers (Brachionusplicatilis).* s.l.:Aquaculture, 283(1): 102-115.doi.1016/j.aquaculture.2008.06.037.

Fernández, I., Ortiz-Delgado, J., Sarasquete, C. & Gisbert, E., 2012. Vitamin A effects on vertebral bone tissue homeostasis in gilthead sea bream (Sparusaurata) juveniles. *Journal of Applied Ichthyology, 28(3): 419-426.doi:10.1111/j.1439-0426.2012.019.x.*

Fisher, S., Jagadeeswaran, P. & Halpern, M., 2003. *Radiographic analysis of zebrafish skeletal defects.* s.l.:Developmental biology, 264(1): 64-76.doi:10.1016/S0012-1606(03)00399-3.

FishStat, Accessed 2019. *http://www.fao.org/fishery/statistics/en,* s.l.: s.n.

Fjelldal, et al., 2006. Impact of smolt production strategy on vertebral growthand mineralisation during smoltification and the early sea water phase in Atlantic Salmon (Salmo salar, L.). Aquaculture. In: s.l.:s.n., pp. 715-728.

Folkestad, A. et al., 2008. Rapid and non-invasive measurements of fat and pigment concentrations in live and slaughtered Atlantic salmon (Salmo salar L.). *Aquaculture,* 280(1), p. DOI: 10.1016/j.aquaculture.2008.04.037.

Fondriest Environmental, 2013. *Fundamentals of Environmental Measurements,* s.l.: https://www.fondriest.com/environmental-measurements/parameters/water-quality/dissolved-oxygen/.

Forandriest environmental products, 2017. *https://www.fondriest.com/environmental-measurements/parameters/water-quality/dissolved-oxygen/,* s.l.: s.n.

Gavaia, P. J., Sarasquete, C. & Cancela, M. L., 2000. *Detection of mineralized structures in early stages of development of marine Teleostei using a modified alcian blue-alizarin red double staining technique for bone and cartilage, Biotech Histochem, 7,* s.l.: s.n.

Georgakopoulou, E., Katharios, P., Divanach, P. & Koumoundouros, G., 2010. *Effect of temperature on the development of skeletal deformities in Gilthead seabream (Sparusaurata Linnaeus, 1758).* s.l.: Aquaculture, 308(1): 13-19.doi:10.1016/j.aquaculture.2010.08.006.

Gjedrem, T., Gjøen, M. H. & Gjerde, B., 1991. Genetic origin of Norwegian farmed Atlantic salmon. *Aquaculture,* 98(1-3), pp. 41-50.

Gjerde, B., Pante, M. & Baeverfjord, G., 2005. Genetic variation for a vertebral deformity in Atlantic salmon (Salmo salar). *Aquaculture,* 244(1-4), pp. 77-87DOI: 10.1016/j.aquaculture.2004.12.002.

Gjerde, B., Sonesson, A., Storset, A. & Rye, M., 2007. Selective Breeding and Genetics-Atlantic Salmon. In: *Aquaculture- Production of Aquatic Organisms(2000-2005).* Oslo: PDC Tangen, pp. 268-284.

Gjøen, H. M. & Bentsen, H. B., 1997. Past, present, and future of genetic improvement in salmon aquaculture. *ICES Journal of Marine Science,* 54(6), pp. 1009-1014.

Haga, Y., Suzuki, T., Kagechika, H. & Takeuchi, T., 2003. A retinoic acid receptor-selective agonist causes jaw deformity in the Japanese flounder, Paralichthysolivaceus. *Aquaculture,* pp. 221: 381–392 doi:10.1016/S0044-8486(03)00076-0..

Haga, Y., Suzuki, T., Kagechika, H. & Takeuchi, T., 2003. *A retinoic acid receptor-selective agonist causes jaw deformity in the Japanese flounder, Paralichthysolivaceus.* s.l.:Aquaculture, 221: 381–392.doi:10.1016/S0044-8486(03)00076-0.

Hansen, T., 2019 pdf. Laksens virvelsøyle og deformasjoner. *Havforskingintituttet, Institute of Marine Research.*

Hard, J. J. et al., 2008. Evolutionary consequences of fishing and their implications for salmon.. *Evolutionary applications*, 1(2), pp. 388-408 doi:10.1111/j.1752-4571.2008.00020.x.

Heisinger, J. & Green, W., 1975. *Mercuric chloride uptake by eggs of the ricefish and resulting teratogenic effects.* s.l.:Bulletin of Environmental Contamination and Toxicology, 14: 665–673.doi:10.1007/BF01685240.

Helland, S. et al., 2005. Mineral balance and bone formation in fast-growing Atlantic salmon parr (Salmo salar) in response to dissolved metabolic carbon dioxide and restricted dietary phosphorus supply. *Aquaculture,* Volume 250, p. 346–376.

Herbinger, C. M. et al., 1995. DNA fingerprint based analysis of partenal and martenal effects on offspring growth and survival in communally reared rainbow trout. *Aquaculture,* Volume 137, pp. 245-256.

Hofer, A., 1998. Variance component estimation in animal breeding: a review†. 115(1-6), pp. 247-265 doi:10.1111/j.1439-0388.1998.tb00347.x.

Hsieh, J., 2015. *Computed Tomography: Principles, Design, Artifacts, and Recent Advances.* Third ed. s.l.:ISBN: 9781628418255.

Johansson, L.-H.et al., 2016. Smoltification and seawater transfer of Atlantic salmon (Salmo salar L.) is associated with systemic repression of the immune transcriptome. *Fish and Shellfish Immunology,* Issue 58, pp. 33-41.

Kak, A. C. & Slaney, M., 1988. *Principles of Computerized Tomographic Imaging.* s.l.:IEEE Press.

Kalender, W. A., 2005. *Computed Tomography: Fundamentals, System Technology, Image Quality, Applications.* Third ed. s.l.:ISBN: 978-3-895-78317-3.

Kause, A. et al., 2010. Quality and production trait genetics of farmed European whitefish, Coregonus lavaretus. *Journal of Animal Science,* J Anim Sci 2011.89:959-971(doi: 10.2527/jas.2010-2981).

Kause, A., Quinton, C. D., Ruohonen, K. & Koskela, J., 2007. Genetic relationships of body composition and feed utilization traits in European whitefish (Coregonus lavaretus L.) and implications for selective breeding in fishmeal- and soybean meal-based diet environments. *Journal of Animal Science,* doi:10.2527/jas.2006-792(J. Anim. Sci. 2007. 85:3198–3208).

Kihara, M. et al., 2002. *Lordosis induction in juvenile red sea bream, Pagrus major, by high swimming activity.* s.l.:Aquaculture, 212: 149–158.doi:10.1016/S0044-8486(01)00871-7.

Klemsten, A. et al., 2003. Atlantic salmon Salmo salar L., brown triut Salmo trutta L. and Arctic charr Salvelinus alpinus(L.): a review of aspects of their histories. In: *Ecology of Freshwater Fish.* Copenhagen: Blackwell Munksgaard, pp. 1-59.

Kongtorp, R. T., Halse, M., Taksdal, T. & Falk, K., 2006. Longitudinal study of a natural outbreak of heart and skeletal muscle inflammation in Atlantic salmon, Salmo salar L.. *Journal of Fish Diseases,* 29(4).

Kyung Joon, K. et al., 2019. Hounsfield Units on Lumbar Computed Tomography for Predicting Regional Bone Mineral Density. *Open medicine,* Volume 14 , pp. 545–551 doi: 10.1515/med-2019-0061.

Lall, S. P., 2002. The minerals. In: J. Halver & R. Hardy, eds. *Fish Nutrition.* 3rd ed. San Diego: Academic Press Inc, pp. 259–308.doi:10.1016/B978-012319652-1/50006-9..

Lim, C. & Lowell, R., 1978. Pathology of the vitamin C syndrome in channel catfish (Ictalurus punctatus) . J Nutr. 108:([PubMed]), p. 1137–1146.

Madsen, L. & Dalsgaard, I., 1999. *Vertebral column deformities in farmed rainbow trout (Oncorhynchusmykiss).* s.l.:Aquaculture, 171(1): 41-48.doi:10.1016/S0044-8486(98)00427-X.

Mahamid, J. S. A. A. L. W. S., 2008. *Amorphous calcium phosphate is a major component of the forming fin bones of zebrafish: indications for an amorphous precursor phase.* s.l.: Proceedings of the National Academy of Sciences, 105(35): 12748-12753.doi:10.1073/pnas.0803354105.

Marine Institute, 2019. *https://www.marine.ie/Home/site-area/areas-activity/fisheries-ecosystems/salmon-life-cycle,* s.l.: © Marine Institute.

Marty-Mahé, P. et al., 2004. *Quality traits of brown trout (Salmo trutta) cutlets described by automated color image analysis,* doi: 10.1016/S0044-8486(03)00458-7: Aquaculture, 232 (1): 225-240.

Meuwissen T, 1997. *Optimal Contributions procedures in fish breeding designs,* s.l.: s.n.

Moro, L. et al., 2000. *Posttranslational modifications of bone collagen type 1 are related to the function of rat femoral regions.* s.l.:Calcified Tissue International, 66: 151-156.doi:10.1007/s002230010030.

Muramoto, S., 1981. *Vertebral column damage and decrease of calcium concentration in fish exposed experimentally to cadmium, Environmental Pollution Series A.* s.l.:Ecological and Biological, 24(2): 125-133.doi:10.1016/0143-1471(81)90074-X.

Norwegian Sea Food Council, 2018. *https://www.salmon.fromnorway.com/,* s.l.: s.n.

NS9401, 1994. *Atlantic Salmon.,* s.l.: Reference Sampling for Quality Measurements. Norwegian.

OECD, 2017. “Atlantic salmon (Salmo salar)”, in Safety Assessment of Transgenic Organisms in the Environment. Volume 7: OECD Consensus Documents(OECD Publishing, Paris), pp. 107-239 : DOI: https://doi.org/10.1787/9789264279728-7-en.

Oldenbroek, K. & Waaij, L. v. d., 2014. *Animal breeding and genetics for BSc Students.* Netherlands: Centre for Genetic Resources and Animal Breeding and Genomics group,Wageningen University and Research Centre.

Oldenbroek, K. & Waaij, L. v. d., 2015. *Animal Breeding and Genetics.* https://wiki.groenkennisnet.nl/x/p4AI ed. s.l.:Animal Breeding and Genomics Centre (ABGC) of Wageningen UR (University and Research Centre).

Ottani, V. et al., 1998. Collagen fibril arrangement and size distribution in monkey oral mucosa. *Journal of Anatomy, 192: 321–328.doi: 10.1046/j.1469-7580.1998.19230321.x.*.

Oxford Reference, accessed 2019. *https://www.oxfordreference.com/view/10.1093/oi/authority.20110803095946588.*, s.l.: s.n.

Per Gunnar Fjelldal, et al., 2006. Impact of smolt production strategy on vertebral growth and mineralisation during smoltification and the early seawater phase in Atlantic salmon ( Salmo salar, L). *Per Gunnar Fjelldal,* Volume 261, pp. 715-728.

Piotrowski, T. et al., 1996. *JAw and branchial arch mutants in zebrafish II.* s.l.:anterior arches and cartilage differentiation, Development, 123(1):345-356.

Press, 1957. *The Effects of Atomic Radiation on Oceanography and Fisheries, Extract from The National Academies,* Washington DC: The National Academies Press.

Rasband, W., 1997-2015. *ImageJ:http://imagej.nih.gov/ij,* Bethesda, Maryland, USA: National institutes of Health.

Robertson, A. & Lerner, I. M., 1949. The Heritability of All-or-None TraitsViability of Poultry. *Genetics,* 34(4), pp. 395-411.

Rosa-Molinar, E., Proskocil, B. J., Ettel, M. & & Fritzsch, B., 1999. Whole-mount procedures for simultaneous visualization of nerves, neurons, cartilage and bone.. *Brain Res Protoc,* 4(2), pp. 115-123 doi:10.1016/s1385-299x(99)00007-0.

Rosenthal, N. E. et al., 1989. Psychobiological effects of carbohydrate- and protein-rich meals in patients with seasonal affective disorder and normal controls.. *Biological Psychiatry,* 25(8), pp. 1029-1040 doi:https://doi.org/10.1016/0006-3223(89)90291-6..

Roy, P. & Lall, S., 2003. *Dietary phosphorus requirement of juvenile haddock (Melanogrammusaeglefinus L.).* s.l.:Aquaculture, 221: 451–468.doi:10.1016/S0044-8486(03)00065-6.

Roy, P. & Lall, S., 2007. *Vitamin K deficiency inhibits mineralization and enhances deformity in vertebrae of haddock (Melanogrammusaeglefinus L.). Comparative Biochemistry and Physiology Part B: Biochemistry and Molecular Biology, 148(2): 174-183.doi:10.1016/i.cbpb.2007.05.006.* s.l.:s.n.

Sakamoto, W. et al., 2000. Mitochondrial localization of AtOXA1, an arabidopsis homologue of yeast Oxa1p involved in the insertion and assembly of protein complexes in mitochondrial inner membrane.. *Plant Cell Physiol,* 41(10), pp. 1157-1163 doi:10.1093/pcp/pcd045.

Sambraus, F. et al., 2014. Vertebra deformities in wild Atlantic salmon caught in the Figgjo River, southwest Norway. *Journal of Applied Ichthyology ,* 30(4), p. DOI: 10.1111/jai.12517.

Sarnowski, P., 1998. The effect of copper on grass carp larvae. In: *2nd international conference Trace Elements: Effects of organisms and environment.* s.l.:Katowice, pp. 181-185.

Schilling, T. et al., 1996. *Jaw and branchial arch mutants in zebrafish I.* s.l.:branchial arches, Development, 123(1):329-344.

Sea food from Norway, accessed 2018. *https://fromnorway.com/learn-more/seafood-encyclopedia/salmon/,* s.l.: s.n.

Sfakianakis, D. G. E. et al., 2006. *Environmental determinants of haemallordosis in European sea bass, Dicentrarchuslabrax (Linnaeus, 1758).* s.l.:Aquaculture, 254(1): 54-64.doi:10.1016/j.aquaculture.2005.10.028.

Sharber, N. & Carothers, S., 1988. *Influence of electrofishing pulse shape on spinal injuries in adult rainbow trout, North American Journal of Fisheries Management, 8(1): 117-122.doi:10.1577/1548-8675(1988)008<0117:IOEPSO>2.3.CO;2.* s.l.:s.n.

Skaarud A, W. J. A. G. H. M., 2003. Strategies for controlling inbreeding in fish breeding programs;an applied approach using optimum contribution (OC) procedures. *Aquaculture 311,* pp. 110-114.

Skrede, G. & Wold, J.-P., 2008. Colour Quality of Salmon. In: *ASC symposium series.* Washington DC: American Chemical Society, pp. 242-252.

Somasundaram, B., King, P. & Shackley, S., 1984. *The effects of zinc on postfertilization development in eggs of Clupea harengus L.* s.l.:Aquatic Toxicology, 5: 167–178. doi:10.1016/0166-445X(84)90007-9.

Sprawls Educational Foundation, Acessed 2019. *Open resources for learning and teaching, The physical principles of medical imaging,* s.l.: http://www.sprawls.org/resources/CTIMG/module.htm.

Standards, 1969. *Coturnix (Coturnix Coturnix Japonica): Standards and Guidelines for the Breeding, Care, and Management of Laboratory Animals,* s.l.: A Report: National Academy of Sciences.

Summers, A., 2015. *The Compleat Guide to Clearing and Staining.,* s.l.: s.n.

Takeuchi, T. et al., 1998. *Effect of vitamin A compounds on bone deformity in larval Japanese flounder (Paralichthysolivaceus).* s.l.:Aquaculture, 169: 155–165.doi:10.1016/S0044-8486(98)00373-1.

Tave Douglas, 1986. *Genetics for fish hatcheries managers.* ISBN:0870555324, 9780870555329 ed. Michigan: AVI Pub. Co., .

The sustainable trade initiative, accessed 2018. *https://salmonfacts.com/fish-farming-in-norway/how-is-farmed-salmon-treated/,* s.l.: s.n.

Verspoor, E., Stradmeyer, L. & Nielsen, J. L., 2008. *The Atlantic Salmon: Genetics, Conservation and Management ,* s.l.: Wiley..

Whitehouse, R. & Adams, J., 1992. (1992). Single energy quantitative computed tomography: The effects of phantom calibration material and kVp on QCT bone densitometry.. *The British journal of radiology,* Volume 65, pp. 931-934 doi:10.1259/0007-1285-65-778-931.

Witten, P. et al., 2005. Compressed vertebrae in Atlantic salmon Salmo salar: evidence for metaplastic chondrogenesis as a skeletogenic response late in ontogeny.. *Diseases of aquatic organisms,* 64(3), pp. 237-246.

X-Rite, I., 2019. EU-EN: Accessed November, 2019.

# 8 Appendices

Appendix A

Open the application, drag and drop an image on the open tab.

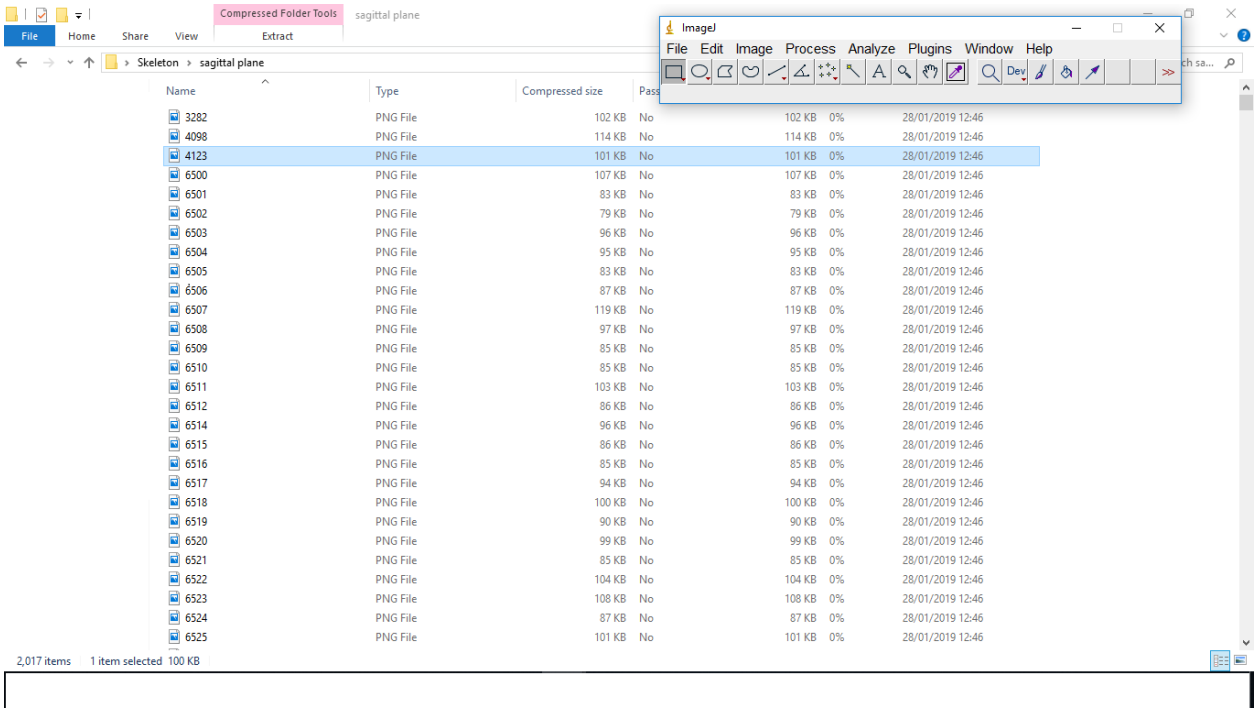

Once the image is open, select a tool that you need to draw along the vertebral column.

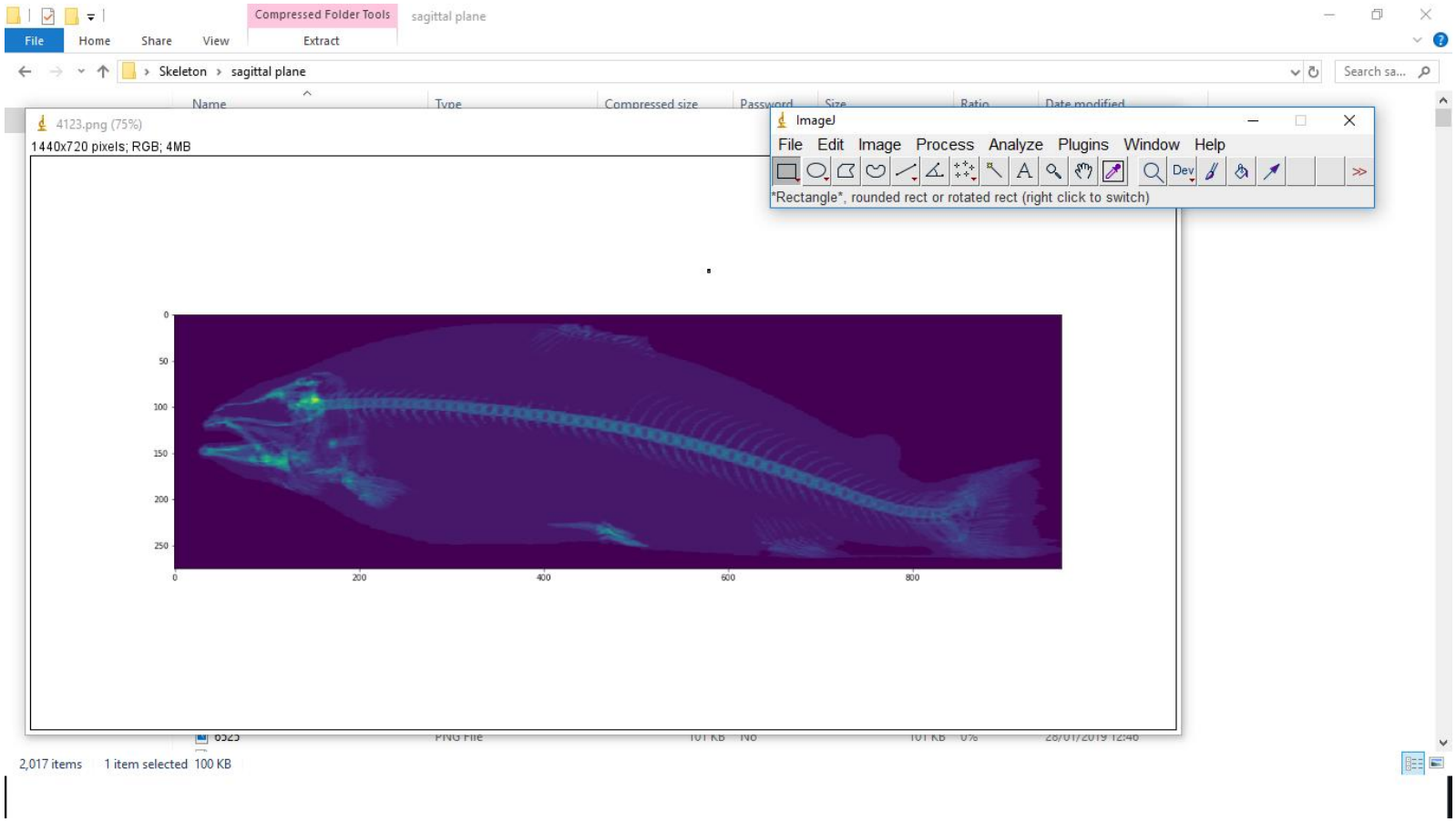

Draw or select a section of approximately 2-5 vertebrae in the regions from A to E. click on plugins, then analyse, then RGB measure.

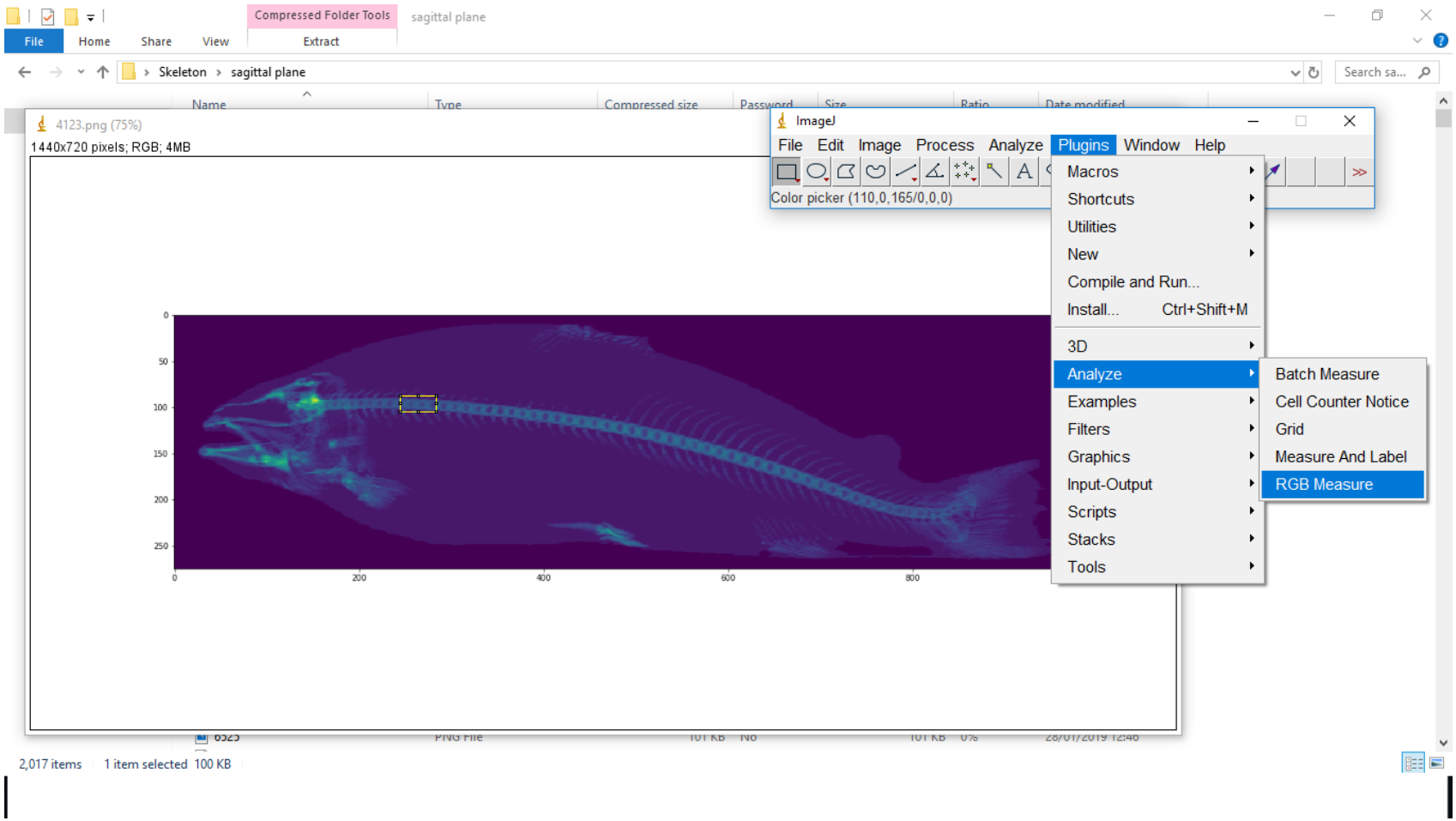

This measures the values of the colorimetric value of the bone as RGB space in the different regions and the area calculated is shown by the mean value from the programme.

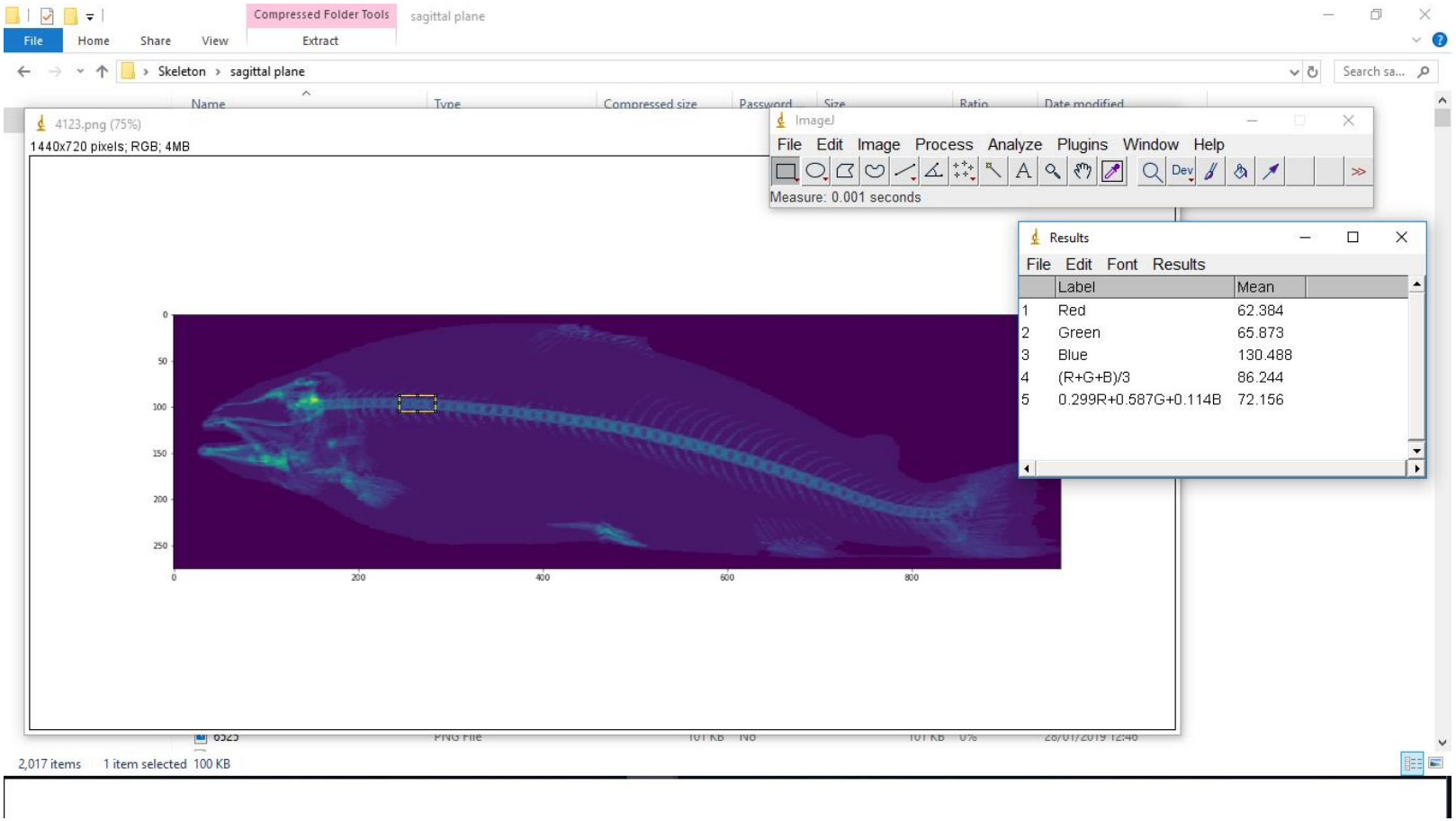

Appendix B

| | | Anterior 1 (Region A) | Anterior 2 (Region B) | Mid 3 (Region C) | Post 4 (Region D) | Post 5 (Region E) | Soft bone (1) | Jaw (2) | Muscle (3) |
|---|---|---|---|---|---|---|---|---|---|
| high-low | L*-value | 5 | 4 | 2 | 3 | 6 | 7 | 1 | 8 |
| low-high | a*-value | 5 | 4 | 2 | 3 | 6 | 7 | 1 | 8 |
| high-low | b*-value | 5 | 4 | 2 | 3 | 6 | 8 | 1 | 7 |

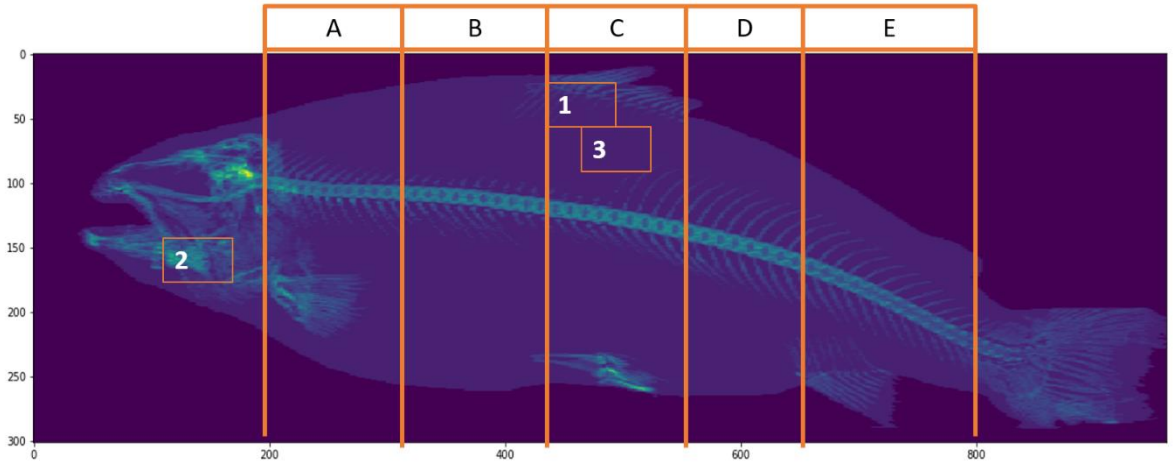

Appendix C

The MEANS Procedure (n=1176)

Position=Ant_1(Region A)

| Variable | Mean | Minimum | Maximum | Std Error | Std Dev | Coeff of Variation |
|---|---|---|---|---|---|---|
| **ID** | 7915.73 | 6500.00 | 10066.00 | 27.73 | 951.05 | 12.01 |
| **L*Value** | 34.39 | 28.04 | 48.38 | 0.07 | 2.50 | 7.28 |
| **a*Value** | 10.99 | -19.83 | 25.08 | 0.17 | 5.83 | 53.08 |
| **b*Value** | -34.78 | -39.50 | -14.59 | 0.08 | 2.74 | -7.88 |

Position=Ant_2 (Region B)

| Variable | Mean | Minimum | Maximum | Std Error | Std Dev | Coeff of Variation |
|---|---|---|---|---|---|---|
| **ID** | 7915.73 | 6500.00 | 10066.00 | 27.73 | 951.05 | 12.01 |
| **L*Value** | 35.76 | 29.30 | 51.68 | 0.08 | 2.68 | 7.51 |
| **a*Value** | 7.52 | -26.48 | 21.98 | 0.18 | 6.15 | 81.75 |
| **b*Value** | -33.08 | -38.99 | -9.23 | 0.09 | 3.16 | -9.57 |

Position=Mid_3 (Region C)

| Variable | Mean | Minimum | Maximum | Std Error | Std Dev | Coeff of Variation |
|---|---|---|---|---|---|---|
| **ID** | 7915.73 | 6500.00 | 10066.00 | 27.73 | 951.05 | 12.01 |
| **L*Value** | 37.56 | 29.73 | 55.35 | 0.09 | 2.92 | 7.79 |
| **a*Value** | 3.23 | -32.901 | 21.03 | 0.19 | 6.58 | 203.97 |
| **b*Value** | -30.82 | -38.61 | -2.17 | 0.11 | 3.70 | -12.01 |

Position=Post_4 (Region D)

| Variable | Mean | Minimum | Maximum | Std Error | Std Dev | Coeff of Variation |
|---|---|---|---|---|---|---|
| **ID** | 7915.73 | 6500.00 | 10066.00 | 27.73 | 951.05 | 12.01 |
| **L*Value** | 37.09 | 29.82 | 54.54 | 0.08 | 2.88 | 7.76 |
| **a*Value** | 4.18 | -31.58 | 21.36 | 0.19 | 6.48 | 155.28 |
| **b*Value** | -31.27 | -38.65 | -3.87 | 0.10 | 3.56 | -11.39 |

Position=Post_5 (Region E)

| Variable | Mean | Minimum | Maximum | Std Error | Std Dev | Coeff of Variation |
|---|---|---|---|---|---|---|
| **ID** | 7915.73 | 6500.00 | 10066.00 | 27.73 | 951.05 | 12.01 |
| **L*Value** | 33.39 | 26.18 | 50.28 | 0.09 | 2.97 | 8.90 |
| **a*Value** | 13.02 | -23.43 | 29.39 | 0.20 | 6.94 | 53.27 |
| **b*Value** | -35.42 | -40.39 | -12.70 | 0.09 | 2.97 | -8.39 |

Position=Softb_6 (Soft Bone)

| Variable | Mean | Minimum | Maximum | Std Error | Std Dev | Coeff of Variation |
|---|---|---|---|---|---|---|
| **ID** | 7915.73 | 6500.00 | 10066.00 | 27.73 | 951.05 | 12.01 |
| **L*Value** | 22.52 | 20.23 | 28.32 | 0.03 | 0.99 | 4.39 |
| **a*Value** | 35.40 | 25.46 | 37.98 | 0.04 | 1.35 | 3.81 |
| **b*Value** | -39.67 | -40.62 | -38.31 | 0.01 | 0.42 | -1.07 |

Position=Strong_7 (Jaw)

| Variable | Mean | Minimum | Maximum | Std Error | Std Dev | Coeff of Variation |
|---|---|---|---|---|---|---|
| **ID** | 7915.73 | 6500.00 | 10066.00 | 27.73 | 951.05 | 12.01 |
| **L*Value** | 42.25 | 29.59 | 62.60 | 0.13 | 4.41 | 10.45 |
| **a*Value** | -7.23 | -43.88 | 21.64 | 0.27 | 9.28 | -128.41 |
| **b*Value** | -23.86 | -38.59 | 15.70 | 0.20 | 6.78 | -28.42 |

Position=Muscle_8 (Muscle)

| Variable | Mean | Minimum | Maximum | Std Error | Std Dev | Coeff of Variation |
|---|---|---|---|---|---|---|
| **ID** | 7915.73 | 6500.00 | 10066.00 | 27.73 | 951.05 | 12.01 |
| **L*Value** | 21.27 | 19.22 | 26.44 | 0.03 | 0.86 | 4.05 |
| **a*Value** | 37.01 | 29.46 | 38.57 | 0.03 | 0.93 | 2.51 |
| **b*Value** | -39.00 | -40.63 | -37.34 | 0.02 | 0.53 | -1.37 |

Position=Average

| Variable | Mean | Minimum | Maximum | Std Error | Std Dev | Coeff of Variation |
|---|---|---|---|---|---|---|
| **ID** | 7915.73 | 6500.00 | 10066.00 | 27.73 | 951.05 | 12.01 |
| **L*Value** | 33.03 | 27.23 | 46.85 | 0.06 | 2.11 | 6.38 |
| **a*Value** | 13.02 | -14.86 | 25.45 | 0.13 | 4.59 | 35.26 |
| **b*Value** | -33.49 | -38.25 | -14.28 | 0.07 | 2.34 | -6.98 |

# Appendix D

The GLM Procedure

**Dependent Variable: L_Value**

| Source | DF | Sum of Squares | Mean Square | F Value | Pr > F |
|---|---|---|---|---|---|
| **Model** | 7 | 447138.50 | 63876.93 | 8468.96 | <.0001 |
| **Error** | 9400 | 70899.25 | 7.54 | | |
| **Corrected Total** | 9407 | 518037.75 | | | |

| R-Square | Coeff Var | Root MSE | L_Value Mean |
|---|---|---|---|
| 0.8631 | 8.31 | 2.75 | 33.03 |

| Source | DF | Type I SS | Mean Square | F Value | Pr > F |
|---|---|---|---|---|---|
| **Position** | 7 | 447138.50 | 63876.93 | 8468.96 | <.0001 |

**Dependent Variable: b_Value**

| Source | DF | Sum of Squares | Mean Square | F Value | Pr > F |
|---|---|---|---|---|---|
| **Model** | 8 | 210368.79 | 26296.10 | 2261.35 | <.0001 |
| **Error** | 10575 | 122971.16 | 11.63 | | |
| **Corrected Total** | 10583 | 333339.95 | | | |

| R-Square | Coeff Var | Root MSE | b_Value Mean |
|---|---|---|---|
| 0.631094 | -10.18 | 3.41 | -33.49 |

| Source | DF | Type I SS | Mean Square | F Value | Pr > F |
|---|---|---|---|---|---|
| **Position** | 8 | 210368.79 | 26296.10 | 2261.35 | <.0001 |

Appendix E

The genetic correlations for L*values on the bottom side of the diagonal, the multivariate heritability on the diagonal and the phenotypic correlations above the diagonal.

| | **Region A** | **Region B** | **Region C** | **Region D** | **Region E** | **Soft Bone** | **Jaw** | **Muscle** |
|---|---|---|---|---|---|---|---|---|
| **Region A** | **0.23 (0.05)** | 0.83* | 0.83* | 0.79* | 0.72* | 0.74* | 0.41* | 0.78* |
| **Region B** | 0.99 (0.02) | **0.3 (0.06)** | 0.85* | 0.80* | 0.71* | 0.75* | 0.42* | 0.80* |
| **Region C** | 0.97 (0.02) | 0.98 (0.02) | **0.32 (0.06)** | 0.86* | 0.73* | 0.77* | 0.43* | 0.82* |
| **Region D** | 0.99 (0.01) | 0.98 (0.02) | 0.99 (0.01) | **1 (NE)** | 0.79* | 0.75* | 0.43* | 0.80* |
| **Region E** | 0.94 (0.05) | 0.98 (0.05) | 0.96 (0.05) | 0.98 (0.04) | **0.13 (0.04)** | 0.62* | 0.51* | 0.69* |
| **Soft Bone** | 1 (0.03) | 0.92 (0.04) | 0.90 (0.04) | 0.94 (0.03) | 0.96 (0.06) | **0.26 (0.06)** | 0.38* | 0.92* |
| **Jaw** | 0.54 (0.18) | 0.62 (0.16) | 0.56 (0.17) | 0.52 (0.17) | 0.53 (0.21) | 0.61 (0.17) | **0.09 (0.04)** | 0.37* |
| **Muscle** | 1 (NE) | 0.95 (0.03) | 0.94 (0.03) | 0.96 (0.03) | 0.95 (0.06) | 0.98 (0.01) | 0.54 (0.18) | **0.26 (0.06)** |

Appendix F

The genetic correlations for b*values are shown below the diagonal, the multivariate estimates of heritability on the diagonal and the phenotypic correlations above the diagonal.

| | **Region A** | **Region B** | **Region C** | **Region D** | **Region E** | **Soft Bone** | **Jaw** | **Muscle** |
|---|---|---|---|---|---|---|---|---|
| **Region A** | **0.23 (0.05)** | 0.83* | 0.86* | 0.84* | 0.76* | -0.70* | 0.44* | -0.75* |
| **Region B** | 0.99 (0.02) | **0.32 (0.06)** | 0.89* | 0.86* | 0.77* | -0.71* | 0.46* | -0.77* |
| **Region C** | 0.97 (0.02) | 0.98 (0.01) | **0.32 (0.06)** | 0.90* | 0.78* | -0.73* | 0.46* | -0.79* |
| **Region D** | 0.97 (0.02) | 0.98 (0.01) | 0.99 (0.01) | **1 (NE)** | 0.83* | -0.71* | 0.47* | -0.78* |
| **Region E** | 0.96 (0.04) | 0.98 (0.04) | 0.96 (0.04) | 1 (0.03) | **0.14 (0.04)** | -0.57* | 0.53* | -0.66* |
| **Soft Bone** | -1 (NE) | -0.96 (0.04) | -0.92 (0.04) | -0.95 (0.36) | -1 (NE) | **0.27 (0.06)** | -0.35* | 0.91* |
| **Jaw** | 0.59 (0.17) | 0.63 (0.15) | 0.6 (0.15) | 0.58 (0.15) | 0.63 (0.17) | -0.68 (0.15) | **0.11 (0.04)** | -0.37* |
| **Muscle** | -0.99 (0.03) | -0.98 (0.02) | -0.94 (0.03) | -0.97 (0.03) | -1 (NE) | 0.96 (0.03) | -0.63 (0.16) | **0.27 (0.06)** |


**Norges miljø- og biovitenskapelige universitet**
Noregs miljø- og biovitskapelege universitet
Norwegian University of Life Sciences

Postboks 5003
NO-1432 Ås
Norway